JOINT FREQUENCY ALLOCATION AND POWER CONTROL FOR MINIMUM DOWNLINK INTERFERENCE IN FEMTOCELLULAR NETWORKS

A Thesis

by

Gülden Ferazoğlu

Submitted to the
Graduate School of Sciences and Engineering
In Partial Fulfillment of the Requirements for
the Degree of

Master of Science

in the
Department of Electrical and Electronics Engineering

Özyeğin University
January 2013

JOINT FREQUENCY ALLOCATION AND POWER CONTROL FOR MINIMUM DOWNLINK INTERFERENCE IN FEMTOCELLULAR NETWORKS

Approved by:

Professor M. Oğuz Sunay, Advisor
Department of Electrical and Electronics Engineering
Özyeğin University

Professor Ali Özer Ercan
Department of Electrical and Electronics Engineering
Özyeğin University

Professor İsmail Arı
Department of Computer Science
Özyeğin University

Date Approved: 7 January 2013

To my family,

Salih, Gülay and Gizem

ABSTRACT

Due to the fact that the most of data services and more than half of calls are requested indoors, it has been dramatically important and even a must for cellular operators to provide more than adequate indoor coverage. Instead of expensive traditional approach which is to use outdoor macrocell base stations to provide good indoor coverage, indoor systems deployed and installed by operators such as picocells are proposed first. However, these solutions are still too expensive for the cases of small offices and homes where only a few indoor users are there, even though they are found desirable and feasible in hotspots, large business centres and malls.

Femtocell as home base station is one of the developing technologies as a recent solution to aforementioned problems. They offer to improve the indoor coverage and reduce the cellular network load as well as providing broadband data services. However, in case of the most feasable solution, co-channel deployment of the femtocell network over the existing macrocell network, a closed access approach which is more likely to be implemented could result in serious co-channel interference problems.

In this thesis, improvements to the performances of both femtocell and indoor macrocellular users in terms of average achieved data rates are considered. A joint spectrum and power control algorithm is proposed to mitigate the co-tier and cross-tier interferences. The algorithm aims to save the indoor macrocell subscribers from the violation of femtocells whilst providing throughput to femtocell subscribers as higher as possible. Simulations including physical layer and system level are conducted to determine the performance of the proposed method. Results reveal that an algorithm that combines the management of two important resources, spectrum and power, performs really well in two-tier networks, even better than the techniques

managing only one resource, in terms of overall system performance.

ÖZETÇE

Günümüzde veri servislerinin çoğunun ve aramaların da yarıdan fazlasının bina içlerinde talep edildiği gerçeği göz önüne alındığında, hücresel operatörlerin kabul edilebilir seviyenin çok daha üzerinde bina içi kapsama sağlamaları oldukça önemli olmuş, hatta bir zorunluluk haline gelmiştir. İyi seviyede bina içi kapsamanın sağlanması için bina dışı makrohücre baz istasyonlarını kullanmayı öneren geleneksel fakat pahalı yaklaşım yerine, önceleri pikohücreler gibi operatörler tarafından yerleştirilen ve kurulan bina içi sistemler önerilmiştir. Bununla birlikte, bu çözümler her ne kadar büyük iş merkezleri, alışveriş merkezleri gibi hareketli ve kalabalık mekanlarda ilgi çekici ve uygulanabilir görülse de sadece birkaç kişinin bulunduğu küçük ofis ve evler için hala oldukça pahalı ve uygunsuz çözümlerdir.

Söz konusu sorunlara çözüm olarak gelişmekte olan teknolojilerden biri ev baz istasyonu olarak da bilinen femtohücrelerdir. Femtohücreler bina içi kapsamayı iyileştirmek ve hücresel ağ yükünü azaltmak gibi özelliklerinin yanında kullanıcılarına genişbant veri servisleri de sunmaktadırlar. Femtohücre ağının var olan makrohücre ağı üzerine ortak kanal kullanımlı yerleşimi en uygulanabilir çözüm olarak görülmektedir. Ancak böyle bir kurulum durumunda, femtohücrelerde uygulanması en olası olan kapalı erişim yaklaşımı ciddi ortak-kanal girişim problemlerine yol açacaktır.

Bu tezde hem femtohücre hem de bina içlerinde bulunan makrohücre abonelerinin ulaşılan ortalama veri hızları açısından başarımları dikkate alınmıştır. Katman içi (femtohücreler arası) ve katmanlar arası (femtohücre-makrohücre arası) girişimi azaltmak için bir ortak spektrum ve güç kontrolü algoritması önerilmiştir. Önerilen algoritmanın ve dolayısıyla tezin amacı, bina içi makrohücre abonelerinin femtohücre ihlalinden kurtarılması ve veri hızı başarımlarının femtohücre katmanının başarımında

mümkün olan en az kötüleşme ile artırılmasıdır. Önerilen metodun başarımını ölçmek için fiziksel katman ve sistem seviyesini kapsayan benzetimler yapılmıştır. İki-katmanlı hücresel ağlarda iki önemli kaynak olan spektrum ve gücün yönetimini birleştiren bir algoritmanın toplam sistem başarımı açısından oldukça iyi sonuçlar verdiği gözlemlenmiştir. Sonuçlar algoritmanın sadece tek kaynak yönetimi yapan yöntemlerden daha iyi sistem başarımı sağladığını ortaya koymuştur.

ACKNOWLEDGEMENTS

This thesis would not have been possible without the guidance and the help of several individuals who in one way or another contributed and extended their valuable assistance in the preparation and completion of this study.

Foremost, I would like to express my sincere thanks to my advisor Assoc. Prof. M. Oğuz Sunay for his guidance, inspiration and appreciated support during my research. This thesis would not have been completed without his encouragement and advices.

I am also grateful to my friend and project partner Devin Mungan for his friendship, support and belief in me. I could not have imagined having a better project partner. I also thank my fellow labmates in Wireless Information Systems Engineering Research Group: Koray Kökten, Serkan Kırkgül, Volkan Yazıcı and a colleague from Communicatin Theory and Technologies Research Group, Hamza Ümit Sökün, for the inspiring discussions, for the sleepless nights we were working together before deadlines, and for all the fun we have had in the last two years.

The financial support of the Turkish National Science Foundation (TÜBİTAK) is also sincerely acknowledged.

Last but not least, I would like to express my sincere gratitude and profound love to my family: my parents Salih and Gülay Ferazoğlu for supporting me throughout my life and my beloved sister, Gizem, for always being there for me even though I was not able to be with her over the past six years. I thank them for their understanding in hard times and consistent belief in me. Without them, I would not be where I am today.

TABLE OF CONTENTS

LIST OF TABLES

LIST OF FIGURES

CHAPTER I

INTRODUCTION

Due to the increasing consumer demands for mobile data services and higher data rates, cellular networks has been experiencing a major change both topologically and architecturally. With the existing and continuously evolving wireless standards, HSPA and LTE, cellular networks which used to be voice-centric, circuit switched and coverage-considered until recent years, have started to become data-centric, packet switched and naturally deployed for capacity [1]. Mobile data traffic increases exponentially indeed, but also increasing the load on cellular networks. Moreover, according to [2, 3] the majority of these data services is requested indoors. Therefore, providing satisfactory indoor coverage is an important issue for mobile operators. Apparently, it is difficult for cellular networks to solve this indoor coverage problem and cope with the increasing mobile data traffic especially with the expensive and traditional approach of deploying more macro base stations. One of the drawbacks of the traditional solution is the decrease in the overall cell capacity due to the necessity of higher power allocation to the indoor consumers in order to compensate for high penetration losses. Furthermore, the wall penetration is a significant problem for 3G and beyond networks which operate at high frequencies, namely around 2 GHz. Another drawback is that the high order modulation and coding introduced with HSDPA (3G) and beyond require good link qualities to be able to achieve higher data rates. All these problems and still rapidly increasing mobile data traffic has accelerated the development of new innovative technologies.

1.1 Indoor Coverage Solutions

Traditional approach to achieve indoor coverage is deployment of macro base stations, as stated earlier. Service providers should maintain an adequate indoor coverage that fulfil the needs of indoor users and also do not require much investment in expensive traditional solution of macrocell deployment. However, the concept of "adequate" level of indoor capacity has been changed recently due to the expectations of the subscribers on more reliable communication and broadband applications requiring higher data rates. This is how the indoor coverage becomes a problem for providers because deploying more macrocells or increasing transmission power is not a wise solution any more. Therefore, research on this issue has gained importance and several methods have been introduced to overcome the problem [2, 3].

1.1.1 Repeaters

As it is clearly known, wall penetration is one of the most effective factors on the signal attenuation. A repeater is a unit that is developed to amplify the unprocessed signals so that indoor mobile stations could receive adequate power levels. There are two types of repeaters: Passive and active repeaters.

Passive repeaters simply amplify the outdoor signals in a certain frequency band to increase the cellular signal strength inside the house. Main components of a passive repeater are an outdoor antenna, an amplifier and an indoor antenna. Active repeaters on the other hand, are more advanced systems than passive ones. They have also other functionalities such as decoding and re-modifying the signal before retransmission.

The decision of which type of repeater to use is made depending on the environmental requirements. For instance, it is appropriate to use active repeaters in the environments where high error rates are likely while the passive repeaters are usually used in areas only basic amplification operations are required.

1.1.2 Distributed Antenna Systems

A Distributed Antenna System, or DAS, is a network of spatially separated antennas transmitting at low powers which are connected to a common source, an antenna transmitting at higher power. DASs were proposed to provide an indoor radio communication service in [4] since a single central antenna approach is not flexible and reliable due to the various indoor impairments such as signal attenuation and multipath delay spread, specifically for larger buildings.

Essentially, the idea is to split the signal power among spatially separated antenna nodes so that the same area as a single antenna covers is provided with coverage, furthermore the total power is reduced and reliability is enhanced. For more information about DAS, the reader is referred to the references [2, 4].

1.1.3 Small/Indoor Cells

An emerging trend nowadays is to extend the coverage and capacity of a certain service provider with the help of tiered cellular networks which results in the larger cells (macrocells) overlaid with small cells that provide good coverage for a certain number of users. Since the reduced cell size simply results in increasing the wireless throughput [5], indoor base stations were introduced namely picocells, and lately femtocells [6] as a recent solution to overcome the aforementioned problems.

There are considerable differences between picocells and femtocells including coverage and capacity, even though they are both designed as small cells. Firstly, it can be said that they are both dependent upon small smaller base stations with lower power levels and coverage compared to the mBSs (macro base stations). However, a picocell is not subscribers' to install and their deployment locations are planned by the operator as all the other outdoor mBSs. Besides, picocells have larger coverage and capacity than the femtocells, 100m-200m and 10-50 users respectively [2] so that it is not appropriate to call them as home/residential base stations. They may be

suitable for larger covered areas such as malls.

Femtocells, on the other hand, are mostly home or small office owned base stations and they connect to the cellular core network via any Internet connection which is a feature that enables the user installation as it is in Wi-Fi. Therefore, it is not required any installation planning by the provider/operator. Differences between picocells and femtocells summarized and listed in Table 1.

Table 1: Main differences between picocells and femtocells

Criterion	*Picocell*	*Femtocell*
Coverage	100m-200m	<50m
Capacity	10-50 users	3-5 users
Installation	By the service provider	By the subscriber

1.2 Femtocells

Femtocells are typically designed as small in size, low-power, low-cost, user deployed home base stations (Home Node B), also called femtocell access points (FAP) that are connected to the cellular operator network over existing broadband internet back-haul. They simply form a coverage area which is the second tier to the underlaid macro cellular coverage, as illustrated in Figure 1.

Femtocells have some essential characteristics that make them desirable at both the subscriber and the service provider side. Since the distances between a FAP and a subscriber are generally measured in meters, the effects of the wireless channel impairments decrease. Thus, higher signal-to-interference-plus-noise ratio (SINR) becomes achievable for the subscriber unit. Accordingly, it is expected that femtocells provide improved coverage and higher capacity i.e. higher data rates for indoors [6, 7]. This is important because the mobile users of today request bandwidth requiring data services, particularly indoors. Furthermore, femtocells can offer femto-specific

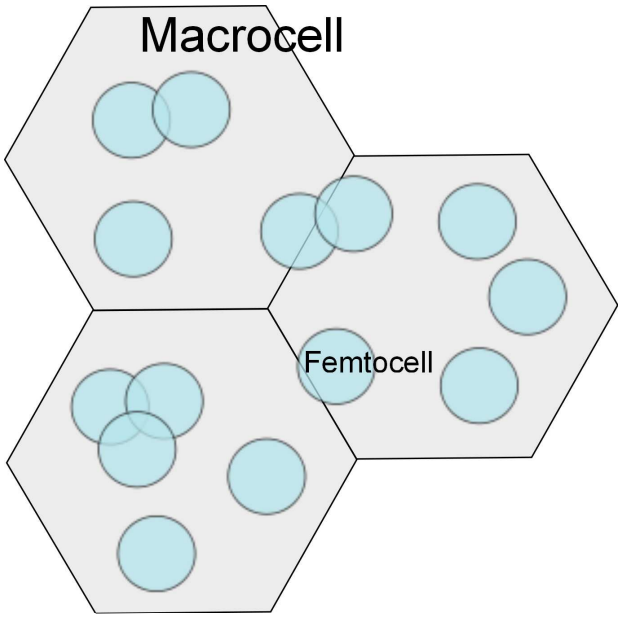

Figure 1: Illustration of a two tiered network

services and other broadband applications to subscribers in the name of providing better service. Longer battery life resulting from short distances between transmitters and receivers is also a considerable benefit for user equipments (UE).

Another important feature of FAPs is the zero-touch feature which implies the "plug and play" manner of FAPs. Accordingly, the user involvement in installing the device should not be necessary. In other words, the initial configuration and the rest of the FAP operation is done automatically without any technical support or user intervention needed.

From the service providers' perspective, femtocell deployment is important concerning the areas that radio access is limited or unavailable. These areas called holes or gaps between macrocells where the users could not receive a signal level sufficient to even make a call, can be covered by femtocells. With the deployment of self-organizing femtocell networks, service provider's indoor coverage problems are also solved with low cost and maintenance instead of macrocell base station's higher cost and expenditure. Offloading indoor connections to a femtocell increases system coverage and capacity allowing the macrocell to provide service to more outdoor cellular

subscribers.

For the reasons aforementioned and more, femtocell nature will attract the attention of both consumers and providers. However, there are also many vital problems with the femtocell technology still need to be addressed and coped with. It is obvious that desired plug and play characteristic of FAPs eventually results in uncoordinated ad-hoc deployment. Due to such unplanned deployment and the facts such as FAP access control type and channel assignment, one of the challenging problems a FAP must deal with, interference, is very likely introduced. Interference results in a decrease in radio system capacity, and hence, interference management techniques are required to mitigate interference which otherwise could degrade the network quality.

1.3 Research Problem

Femtocell networks by nature are exposed to various types of interference. The feature of end user installation resulting in ad-hoc deployment might increase interference to even unacceptable levels. There are different types of interferences based on different scenarios. Several works on interference mitigation are surveyed and presented in section 2.6.

Among all the scenarios, the downlink co-channel operation of closed access femtocells is the most important one since it is more likely to be implemented in reality. As a result, this scenario is studied throughout this thesis. In the co-channel deployment mode a macrocell user equipment (MUE) which is not in the CSG of the femtocell but in the neighbourhood suffers from the high interference and can even lose the network connection from time to time. Moreover, femtocells can also receive significant interference from each other due to the increasing number of FAPs and unplanned deployment.

In this work, we investigate the closed access femtocell overlaid macrocell network for co-channel deployment case and quantify the effect of the proposed joint

spectrum and power management algorithm on the performance of each tier and on the total network throughput. Due to the need of efficient use of limited spectral resources, femtocells must completely reuse the frequency resources particularly when the large number of them are deployed, as well as femtocells and macrocells have to share the frequency bandwidth. In order to deal with the resulting co-tier and cross-tier interferences, an optimum spectrum sensing period is obtained and used without any spectrum partitioning, likewise the independent parameters of the power control scheme, *interference threshold* that denotes the maximum interference level received from all channels a FAP could tolerate and does not reduce its Tx power and *drop percentage* that denotes the percentage of the current transmit power to be reduced, are optimized. Here, with the acquired optimum combination we quantify the enhancement achieved in indoor cellular users' data rate performance with the minimum possible degradation in femtocell tier performance. We also investigate the sensitivity of the optimal solution to the variations in some system parameters.

1.4 Contribution & Thesis Outline

In this thesis, the following contributions are made to solve the aforementioned problems.

1. A quite realistic urban environment model with apartment blocks is built for the simulations so that we have been able to investigate the cases in which femtocell access points could be considerably close to each other. This provides better observing and understanding the problems arising from the user deployment and randomness of the FAPs. Thus, it is pointed out that co-tier interference could be important as cross-tier interference to study.

2. To reinforce the realism of the model, we use the concept of being active and idle for FAPs utilizing the information in a statistical study on mobile information

access. Furthermore, we also take the mobile information access patterns into account.

3. A joint spectrum sensing and power control scheme is proposed for the case of co-channel deployment of closed access femtocells over a macro cellular network. We provide very high spectrum efficiency in this scheme because there is no spectrum partitioning between macrocell and femtocell tiers. Moreover, with power control we intend to maintain a balance between the performances of both indoor cellular users and femtocell users. As a result, it has become possible to provide both power and spectrum saving.

The outline of this thesis is as follows. Chapter II gives the necessary background information on HSDPA extension of WCDMA, interference challenge in two-tiered networks and related work. A novel multi-objective optimized interference mitigation solution over two-tiered femtocell overlaid macrocell HSDPA networks is presented in Chapter III. Then, system-level and simulation-level modellings, descriptions and the assumptions made are given in Chapter IV. Numerical results and performance analysis are presented in Chapter V. Finally, Chapter VI summarizes the concluding remarks.

CHAPTER II

BACKGROUND

2.1 Introduction

After the first results were obtained on the works that exploit electromagnetic waves in communication in late 1890s, analog car phones so-called "the first mobile phones" became quite popular in 1970s. These mobile radio networks were not cellular systems, and capacity of these networks was much lower than that of a cellular network.

Car phone service was succeeded by the first generation of mobile cellular communications systems in the 1980s. Cellular networks allow a division of the coverage area into smaller cells as the name "cellular" implies and thus, provide the concept "frequency reuse" for the first time, leading the capacity increase. The most important and known 1G standards were AMPS (Advanced Mobile Phone System) which is a US standard developed by Bell Laboratories, TACS (Total Access Communication System) which is a UK standard based on the AMPS, and NMT (Nordic Mobile Telephone) initiated in northern Europe [8]. In these first generation systems, analog transmission techniques were used and the main purpose was to transmit voice. Thereafter, the evolution of cellular technology is said to be exponential.

Increasing demands on capacity and quality of service led to the second generation systems take place. The most successful and commonly used 2G systems are GSM (Global System for Mobile Communications), D-AMPS (Digital AMPS), CDMA IS-95, and PDC(Personal Digital Cellular) [8]. 2G cellular systems use digital communications techniques in order to fulfil the needs, since digitization of the analog information brings with it advantages such as enhanced voice capability, higher system capacity and data rates. Since the first aim is better voice transmission again

as it was in 1G systems, 'higher' data rate which is maximum 14.4 kbps is reasonably good for this purpose. However, the *higher* is not higher enough for data services. This is how wireless cellular industry welcomes advanced upgrades which are the technologies known as "Generation 2.5" in the literature, for second-generation systems to enhance the data transmission capabilities of GSM. In general, a 2G system becomes 2.5G with the introduction of at least one of these technologies: HSCSD (High-Speed Circuit-Switched Data), GPRS (General Packet Radio Service), EDGE (Enhanced Data rates for GSM Evolution) and IS-95B. HSCSD provides opportunity for a mobile station to use up to four time slots instead of one for a data connection, thus total rate could be four times the data rate of 2G GSM. However, circuit switched structure of this technology brings some drawbacks such as allocation of timeslots continuously even if there is no data transmission. GPRS, on the other hand, introduces packet switched data services to the existing GSM technology. With GPRS, it is possible for a mobile user to reach a maximum data rate of 160 kbps since GPRS technology provides allocation of up to all eight timeslots to a single user [8]. GPRS is dramatically important in terms of being a stepping stone towards to the next generation.

Another 2.5G technology is EDGE which has a new modulation scheme; 8PSK (Eight Phase Shift Keying) coexisting with the old GMSK (Gaussian Minimum Shift Keying). The combination of EDGE with GPRS is known as Enhanced GPRS (EGPRS) and by this way data rates up to 384 kbps can be achievable. Summing up, 2.5G technologies are enhancements/advanced upgrades to the voice-based 2G systems making them capable for data transmission. After all, in the wireless cellular industry it is required more than just an upgrade: a new generation system. Therefore, Third Generation (3G) systems are designed to provide not only the traditional circuit switched services but broadband data services such as Internet access and multimedia services with high quality images and video streaming/conferencing.

The standardization of 3G systems is carried out by International Telecommunication Union (ITU). In this respect, IMT-2000 (International Mobile Telephony-2000) was proposed by ITU as a global family of specifications for 3G technologies. There are two collaborations of regional standardization bodies established late in the 1990s in order to carry out development and standardization of 3G technology family of IMT-2000. The Third Generation Partnership Project (3GPP) is responsible for the standards UMTS (The Universal Mobile Telecommunications System) and EDGE while the Third Generation Partnership Project 2 (3GPP2) supports CDMA2000 [9]. UMTS 3G standard proposed by the European Telecommunications Standards Institute (ETSI) which is a body of 3GPP, has become a dominant technology especially after the decision of using Wideband Code Division Multiple Access (WCDMA) technology as UMTS air interface. In 3GPP, UMTS is based on the Universal Terrestrial Radio Access (UTRA) of two modes; frequency division duplex (FDD) and time division duplex (TDD). These systems and radio interfaces both are based on spread spectrum radio transmission technology. There are other standards achieving the IMT-2000 requirements and thus approved as members of 3G standard family by ITU such that EDGE, Digital Enhanced Cordless Telecommunications (DECT) standardized by ETSI, and WiMAX (Worldwide Interoperability for Microwave Access) technology.

The standardization process of UMTS begins with Release 99. This release does not include all the features desired and designed for UMTS. Basically, it introduces a GSM core network integrated with WCDMA based radio access network. The process continues with Release 4 which introduces some improvements such as TD-SCDMA, Virtual Home Environment (VHE), and Transcoder-Free Operation (TrFO) [8]. However, Release 5 is considered as the first real 3GPP system because it is this release that makes it possible to provide expected data services and features of a 3G system. Some of these improvements are High Speed Downlink Packet Access

(HSDPA), IP based multimedia services, and end-to-end reliable quality of service for packet switched networks. Afterwards, Release 6 which introduces High Speed Uplink Packet Access (HSUPA), Release 7, and Release 8 which proposes Long Term Evolution (LTE) that is considered as a pre-4G or 3.9G technology are announced. LTE Advanced, on the other hand, is defined as a 4G technology and encompassed in Release 10. The last release of 3GPP is Release 12 of which functional freeze date is in early 2013 [10].

Each generation of cellular standards is defined by new frequency bands, different data rates and radio transmission technologies. While HSDPA as an enhancement to WCDMA provides 14.4 Mbps in the downlink, HSPA+ as an upgrade of HSPA can provide peak data rates up to 168 Mbps in the downlink and 22 Mbps in the uplink theoretically. Furthermore, a recent work [11] for 3GPP on LTE-Advanced referred to as 4G indicates that increased peak data rates are 3 Gbps in the downlink and 1.5 Gbps in the uplink. Nowadays, as a matter of fact, The Fifth Generation (5G) and beyond do not seem so far away to be standardized since many researches and engineers have already begun to work on 5G systems.

The rest of this chapter is organized as follows. In the next section, it is provided a brief information on basics of WCDMA. In Section 2.3 HSDPA technology is addressed since it is used as the 3G cellular system in the simulations. Interference challenge in two tiered networks which are analysed throughout the thesis is given in Section 2.4. Mitigation solutions for different types of interference are presented in Section 2.5 and finally the last section of this chapter presents the related work as the result of conducted literature survey.

2.2 Basics of WCDMA

In mobile cellular systems, consumable resources are limited due to the increasing number of subscribers. Therefore, these systems are designed with the idea of

sharing the resources; time, spectrum and/or the power. This process of sharing takes place with multiple access methods. The multiple access methods known and used globally in 2G and beyond technologies are Frequency Division Multiple Access (FDMA), Time Division Multiple Access (TDMA), and Code Division Multiple Access (CDMA). In FDMA the frequency spectrum is divided into sub-channels and every sub-channel is allocated to a subscriber during the transmission. In TDMA, a subscriber can use all the spectrum but only in the time slots allocated to the subscriber. In CDMA technique, on the other hand, all users can transmit simultaneously utilizing the all frequency spectrum. This time separation is done by the different orthogonal codes assigned to each user.

2.2.1 Spread Spectrum

WCDMA is a multiple access method developed by ETSI and ARIB based on CDMA and as a part of 3GPP standardization it is defined as the radio interface for UMTS. It is a Direct Sequence CDMA (DS-CDMA) technology. In WCDMA, user data bits are spread over a wide bandwidth by multiplying them by pseudo-random spreading sequences that have chip rate much higher than the user data rate. The ratio between the chip rate and user data rate is called the spreading factor (also known as *processing gain*) [12, 8]:

$$SF = R_{chip}/R_{user} \tag{1}$$

The spreading factors used in WCDMA can vary between 4 and 512 whereas the chip rate is constant 3.84 Mcps which determines the bandwidth of the WCDMA system as approximately 5 MHz.

Each user has its own unique spreading code. In both spreading the signal in order to obtain a wideband signal and despreading the wideband signal back to the narrowband signal the same unique code is used. Spreading codes have low cross-correlation with each other. Actually, it is possible to have zero cross-correlation

in the case of fully synchronized orthogonality. This characteristic of the spreading codes allows several wideband signals to coexist on the same radio channel providing high tolerance against narrowband interference. When the mixed wideband signal is correlated with the appropriate spreading code (the one that is also used in spreading) at the receiver, only the desired signal with the corresponding spreading code is despread as all the other wideband signals remain spread. Since the energy of a wideband signal is spread over a very large bandwidth, it is like noise and undetectable compared with the desired signal. Therefore, the desired data can be recovered from the mixed received signal.

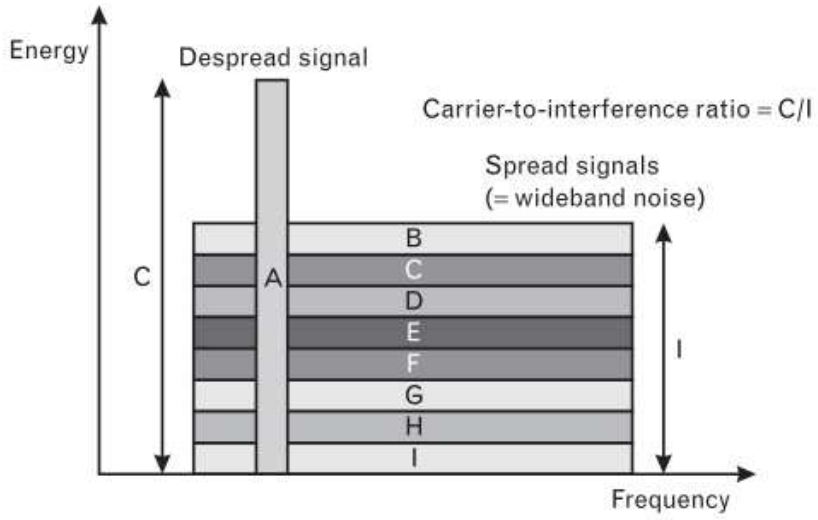

Figure 2: Recovery of despread signal.

2.2.2 Power Control

The concept of power control is crucial for WCDMA network performance. Due to the nature of DS-CDMA technology where all signals are transmitted at the same frequency, it is essential to have a good power control algorithm in the uplink and downlink. The main objective is to transmit the signal with minimal power that is

required for receiver to detect it with adequate quality.

In the uplink direction, the near-far effect is the problem that calls for power control. This problem simply indicates that in the case of all the mobile stations transmit at the fixed power levels, the cells would be dominated by the user close to the base station while the signals of users far away could not be received at the base station. Therefore, in order to avoid the near-far effect, the mobile stations that are far from the base station should transmit with relatively higher power.

In the downlink on the other hand, the reason calling for a downlink power control is interference caused by non-orthogonal signals. It has been stated in the previous subsection that the orthogonal signals which are transmitted one base station in the downlink do not interfere with each other. However, it is not possible to fulfil the requirements of full orthogonality in typical wireless environments due to the impairments such as reflections and scattering. Furthermore, signals transmitted by other base stations are also non-orthogonal and since the neighbouring cells operate at the same downlink frequency in a WCDMA system they also cause an increase in the interference.

Fast power control is obviously one of the most important aspects in a WCDMA system because of the rapid fading due to channel variations. Two main types of power control algorithms are open loop and closed loop power control. In the open loop power control mechanisms, the transmitting side measures the channel interference and changes its transmission power accordingly. This is a fast power control, however it does not give accurate results with UTRA-FDD because of the uncorrelated fast fading between uplink and downlink due to the frequency separation. Instead, the fast closed loop power control (also called the inner loop power control) technique is used both in downlink and uplink in WCDMA (UTRA-FDD) [8, 13]. In this method, the receiver measures the signal to interference ratio (SIR) of the received signal and based on this value, the receiver tells the transmitter to increase or decrease its power.

The closed loop power control in the uplink includes also the outer loop power control which operates within the base station and is responsible for adjusting the target SIR level.

On the whole, the aim is to use the lowest possible transmission power thereby reducing the overall interference level and also decreasing the power consumption.

2.2.3 Soft Handover

The idea of mobility requires mobile stations to maintain their connections in cellular networks when they move from one cell to another. This concept of switching connections between base stations is known as handover (HO). In TDMA systems such as GSM, handover type is hard handover (HHO) which is also known as inter-frequency handover [8] i.e. the transmission on one frequency is stopped before the mobile station moves to another frequency and starts transmission again. In CDMA however, it is introduced soft handover (SHO) where one user equipment (UE) is allowed to be connected to more than one base station (Node B) simultaneously. The nature of WCDMA makes it possible as all Node Bs transmits on the same frequency.

Soft handovers are usually established on the cell boundaries where a UE is able to measure adequately good power levels from more than one cell. If SHO connection is between the adjacent sectors of the same Node B, than it is called softer handover. The set of Node Bs which are the ones the UE establishes a soft/softer HO connection to is known as active set. SHO allows that a UE receives the data from multiple connections in downlink and the data the UE transmits is received from multiple connections in the uplink. The received signals can be combined at both sides which means transmit power levels of both sides can be reduced. Therefore, soft/softer HO decreases overall interference level.

Nevertheless, the SHO should be used with some constraints since every technology has its drawbacks as well as the advantages. Excessive SHO connections may

increase the downlink interference rather than decrease it. Moreover, it can limit the capacity due to the reservation of code resources for one UE from multiple Node Bs.

2.3 High Speed Downlink Packet Access (HSDPA)

High Speed Downlink Packet Access (HSDPA) introduced in 3GPP Release 5 specifications is an extension of WCDMA radio interface, enhancing Release '99 and Release 4 downlink packet data performance in terms of higher peak data rate, lower latency and increased downlink capacity. There are several fundamental techniques introduced in HSDPA to achieve this improvements including Adaptive Modulation and Coding (AMC), channel dependent scheduling, and a fast retransmission strategy (HARQ) [14]. With its uplink counterpart HSUPA introduced in 3GPP Release 6, they form the WCDMA enhancement known as High Speed Packet Access (HSPA) or 3.5G. This section presents necessary background information about HSDPA technology along with the key specifications and techniques which are significant to understand this thesis work.

2.3.1 Introduction

HSDPA technology as a 3G system is designed to provide broadband data services reaching peak data rates up to 14.4 Mbps in downlink. There are several key technical enhancements to the standard WCDMA radio interface to improve downlink packet data in terms of capacity and throughput. The main differences between the HSDPA and the Release 4 are briefly listed below and also shown Table 2 [15].

- The use of shared channel transmission
- Lack of fast power control
- Transmission Time Interval (TTI) of 2ms reducing end user delay
- The use of fast scheduling in Node B

- The use of multiple, up to 15, channels per user
- The introduction of fast transmission techniques and higher order modulations

Table 2: Fundamental differences between HSDPA and Release 4

Feature	*Release*4	*HSDPA*
Fast power control	Yes	No
Adaptive modulation and coding	No	Yes
Multi-code operation	Yes	Yes, extended
Physical layer retransmissions	No	Yes
Link adaptation and BTS based scheduling	No	Yes

2.3.2 Shared Channel Transmission

The use of shared-channel transmission is one of the main characteristics of HSDPA. It is a concept enables that a certain part of total downlink radio resources which are channelization codes and transmission power is dynamically and efficiently shared between users in the time domain. With the implementation of the new shared transport channel, HS-DSCH, in HSDPA it is possible to rapidly allocate a considerable portion of the downlink resources for data transmission to a specific user. This property of the HS-DSCH makes it fit for packet-data applications which are characteristically bursty and thereby have fast varying resource requirements.

The main HS-DSCH code and time sharing structure is illustrated in Figure 3 [14]. The HSDPA code resource is composed of a set of channelization codes of a constant spreading factor 16. The number of codes available for HS-DSCH transmission can be configured from 1 code up to 15 codes for each TTI of 2 ms. The dynamic allocation of these codes to a specific user or several HSDPA users on such a short TTI basis provides an important decrease in the overall delay compared to 10 ms TTI of Release 99 WCDMA. Concerning the link adaptation, it also improves the tracking of rapid channel variations.

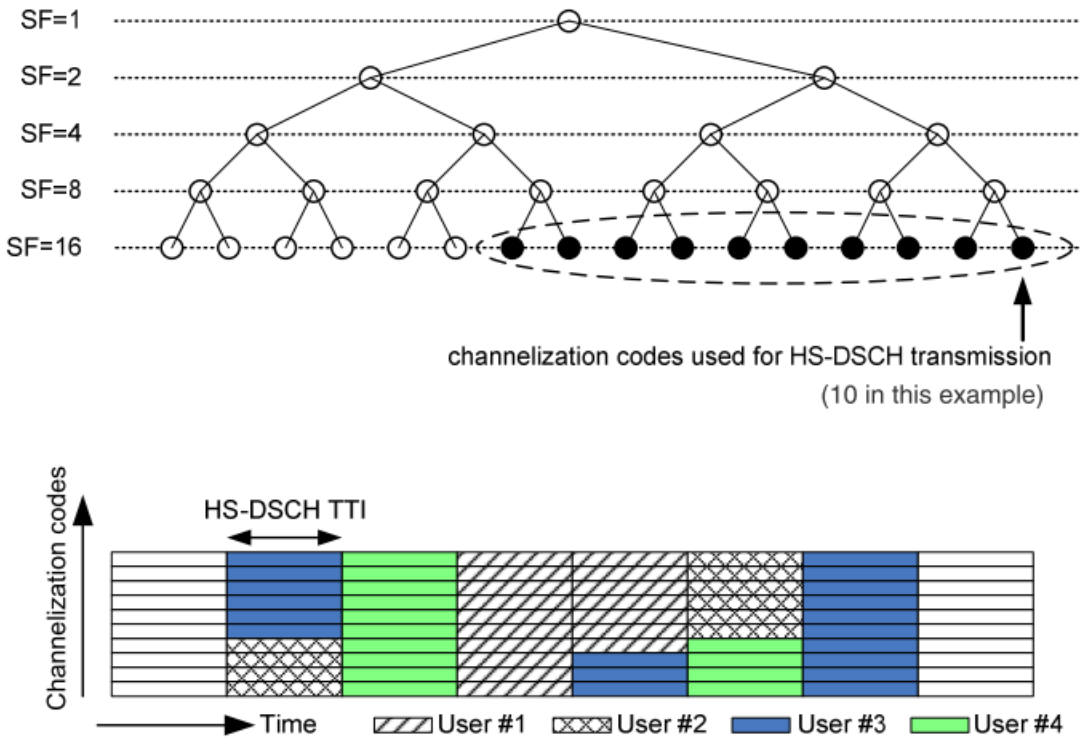

Figure 3: Code and time domain structure of HS-DSCH

Allocation of a certain portion of total cell power for HS-DSCH transmission is also necessary as well as code sharing. This is typically carried out by fast power control in WCDMA which is one of the fundamental features disabled with HSDPA. However, HS-DSCH is rate controlled which allows the remaining power after allocating power to common control and dedicated channels to be used for HS-DSCH transmission. In HSDPA, the adaptation to the fast variations in radio conditions is done by the dynamically changed number of codes, modulation and coding [14, 15]. This link adaptation will be discussed under the section of adaptive modulation and coding.

2.3.3 Adaptive Modulation and Coding

In mobile communications, the dynamics of the environment such as positions of the transmitter and receiver, interference, and other propagation phenomena have a critical role on the changes in the radio channel conditions between Node B and UE.

To be able to track these changes in link quality and to neutralize the effect of these instant variations, concept of link adaptation is introduced. WCDMA implemented link adaptation in the form of power control mechanisms in order to provide reliable communication achieving sufficient energy per information bit for all communication links [14]. In HSDPA however, link adaptation concept is applied using rate control which implies the process of adjusting the downlink bit rate by changing the modulation scheme, coding rate, and number of channelization codes according to the varying radio channel conditions of users. This link adaptation technique is known as adaptive modulation and coding (AMC) and performed by Node B in each TTI based on the link quality reported by the UE.

Each UE sends a channel quality indicator (CQI) message to the Node B at each TTI. The CQI denotes the maximum transport block that the UE could receive at the current channel conditions. CQI values are integers between 0 and 30 where each integer corresponds to measured carrier to interference ratio (CIR) of common pilot channel (C-PICH) [16].

The selection of an effective modulation scheme and coding rate which is referred to as transport format and resource combination (TFRC) for next TTI is done in Node B according to the CQI report sent by the UE. Thus in a system with AMC, users in the favourable positions , i.e. in good link conditions are assigned a higher-order modulation and higher coding rates such as 64QAM/16QAM, 3/4 rate turbo codes whereas a more robust modulation and coding scheme is selected for users with poor channel conditions with the cost of throughput.

Higher amount of multi-codes leads a higher number of downlink code channels used for transmission, hence achieving higher throughput. The maximum number of available multi-codes is 16 with HS-DSCH which is also the spreading code length. However, up to 15 multi-codes can be allocated for one user since one code is reserved for common channels.

There are two different modulation techniques used in Release 5 HSDPA: quadrature phase shift keying (QPSK) and 16 phase quadrature amplitude modulation (16QAM) which is a higher order modulation compared to QPSK that is also used in WCDMA. It is important to note that higher order modulations require a higher signal to interference and noise ratio (SINR). However, for indoor users the received SINR can be so high that the signal quality is not fully utilized even when all available multi-codes, the highest effective coding rate and 16QAM are used [16]. For such particularly good radio channel conditions, the use of 64QAM with HS-DSCH is included in 3GPP Release 7 specifications [17].

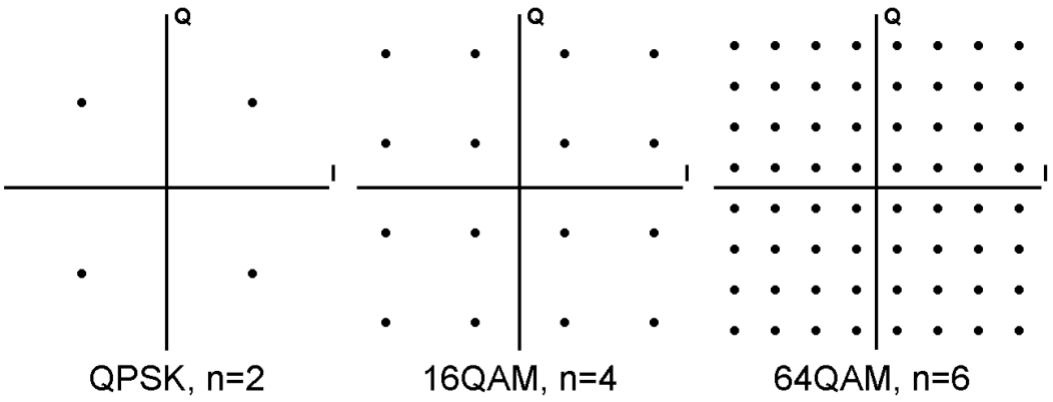

Figure 4: Constellation diagrams for different modulations

Figure 3 represents the constellation diagrams for these three modulation techniques. As it is seen in the figure, more bits per symbol can be sent with 64QAM. However it is more sensitive to symbol errors compared to lower-order modulations since the distance between adjacent symbols are smaller.

Adjustment of the coding rate is another aspect of link adaptation concept to be mentioned. To be able to recover the actual user data stream at the receiver correcting the bit errors occurred due to poor link quality, coding bits are added to the original bit stream. With AMC, coding rate changes to adapt the varying channel conditions. Higher coding protection ensures more error resistant transmission but it

also causes a decrease in the actual throughput since the number of delivered data bits is smaller. In HSDPA, only turbo coding is used for HS-DSCH essentially as convolutional coding can also be used in Release 99 UMTS [15].

TFRC for each UE does not only depends on the radio channel conditions but also the UE capability to support different link adaptation techniques mentioned earlier. All devices may not necessarily support higher-order modulations or more than five channelization codes. Therefore, even in good link conditions, peak data rates a UE can achieve depends on the UE receiver structure. Table 3 lists some of the UE categories specified in 3GPP Release 10 [18] and their supported modulations, maximum number of multi-codes and transport block sizes.

2.3.4 Scheduling

Scheduling has always been a crucial issue in mobile communications since wireless resources are limited and shared between active users. In scheduling, main purpose is that sharing is done as fairly as possible while maximizing the overall system throughput as well.

One of the basic principles of HSDPA is the use of fast scheduling at NodeB which enables the dynamic resource allocation between users with the help of short TTI, 2ms. The scheduling decision of a user is done by a packet scheduler considering different aspects such as CQI report received from the UE, available resources, UE capabilities, data buffer status, and quality of service (QoS). The scheduler can consider all or some of these issues, since the scheduler for HSDPA is not specified by 3GPP and it is vendor specific. However, the common goals of most schedulers are efficient use of HS-DSCH and sharing resources between users fairly.

Maximum carrier-to-interference (Max C/I) scheduler is one of the well-known schedulers used in the cellular communication networks. It tries to achieve maximum

Table 3: HSDPA UE categories

<table>
<tr><th>UE Category</th><th>Max. number of HS-DSCH codes</th><th>Max. number of bits of an HS-DSCH transport block</th><th>Supported modulations without MIMO or aggregated cell operation</th><th>Supported modulations with MIMO and without aggregated cell operation</th></tr>
<tr><td>Category 1</td><td>5</td><td>7298</td><td rowspan="10">QPSK,16QAM</td><td rowspan="14">MIMO not supported</td></tr>
<tr><td>Category 2</td><td>5</td><td>7298</td></tr>
<tr><td>Category 3</td><td>5</td><td>7298</td></tr>
<tr><td>Category 4</td><td>5</td><td>7298</td></tr>
<tr><td>Category 5</td><td>5</td><td>7298</td></tr>
<tr><td>Category 6</td><td>5</td><td>7298</td></tr>
<tr><td>Category 7</td><td>10</td><td>14411</td></tr>
<tr><td>Category 8</td><td>10</td><td>14411</td></tr>
<tr><td>Category 9</td><td>15</td><td>20251</td></tr>
<tr><td>Category 10</td><td>15</td><td>27952</td></tr>
<tr><td>Category 11</td><td>5</td><td>3630</td><td rowspan="2">QPSK</td></tr>
<tr><td>Category 12</td><td>5</td><td>3630</td></tr>
<tr><td>Category 13</td><td>15</td><td>35280</td><td rowspan="2">QPSK, 16QAM, 64QAM</td></tr>
<tr><td>Category 14</td><td>15</td><td>42192</td></tr>
<tr><td>Category 15</td><td>15</td><td>23370</td><td colspan="2">QPSK, 16QAM</td></tr>
<tr><td>Category 16</td><td>15</td><td>27952</td></tr>
<tr><td>Category 19</td><td>15</td><td>35280</td><td colspan="2" rowspan="2">QPSK, 16QAM, 64QAM</td></tr>
<tr><td>Category 20</td><td>15</td><td>42192</td></tr>
</table>

throughput by selecting the users only with a high channel quality to allocate HS-DSCH resources in each TTI. Apparently this is not a scheduler for HSDPA since there is no fairness between users. With max C/I, users with bad signal quality, for instance at cell edge, may never be scheduled. Round-Robin (RR) scheduler on the other hand, aims to allocate radio resources to users equally by selecting them in sequence. However, RR scheduler cannot achieve high throughput because it treats

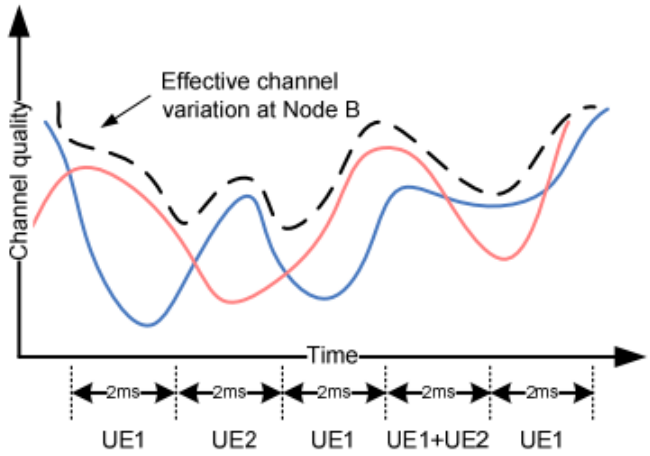

Figure 5: Proportional fair scheduling in HSDPA.

all links in the same way regardless of the CQI feedbacks from the UEs.

There is another well-known scheduling algorithm which is called proportional fair (PF) scheduler. PF scheduler takes into account both goals of improving the expected throughput and providing fair sharing of system resources between users. A relative CQI is calculated for each user using two parameters: achievable data rate at the current TTI and previously received data. Then the user with the highest relative CQI is scheduled [16]. Thanks to this scheduling strategy, PF has become the most popular scheduler used in the HSDPA systems. The basic principle of the PF scheduling is illustrated in Figure 4.

2.3.5 Hybrid ARQ with Soft Combining

The retransmissions of a packet received with errors are controlled by Radio Network Controller (RNC) in Release '99. This causes long delays in data transmission because of the required signalling between the RNC and the Node B. In HSDPA, on the other hand the Node B with a new Medium Access Control (MAC) entity, MAC-hs, located in it is responsible for fast physical layer retransmissions. This fast retransmission strategy is another key technology introduced in HSDPA.

The short retransmission delays of the HSDPA system allow to utilize the previous transmissions for retrieving the original data. For this purpose HSDPA uses hybrid automatic repeat request (HARQ) functionality with soft combining. Soft combining concept implies combining the energy of retransmission(s) with the original transmission of a transport block in order to be able to increase the probability of successfully recovering the transport block [14]. There are two main soft combining techniques in HARQ: Chase Combining (CC) and Incremental Redundancy (IR). In CC [19] the retransmissions are identical to the first transmission. IR on the contrary, is based on non-identical retransmissions of the incorrectly received block. Here, for each retransmissions of the same transport block a different redundancy pattern is used so that every retransmission contains different information.

On the whole, for both methods received erroneous bits are soft combined with the bits from retransmissions at the receiver, the UE, for decoding process. Node B decides to use either one of these CC and IR methods.

A more detailed description of HSDPA principles and the key technologies such as modulation, coding schemes and HARQ functionality can be found in [8, 14, 15].

2.4 Interference Challenge in Tiered Networks

Mobile transmission, by its nature, introduces interference as well as the impairments such as path loss, shadowing and multipath fading. Interference typically occurs when two or more devices are either physically near each other or transmitting on the same or adjacent channels.

As mentioned earlier, FAPs are designed to be deployed indoors to provide service to a few subscribers and cover very small areas compared to mBSs. Femtocell overlaid macrocell networks are referred to as two-tiered networks consisting of macro-tier and femto-tier simultaneously. Such tiered deployments are considered as a solution to

increase overall system capacity, however this tiered deployment is vulnerable to cross-tier interference that occurs between the tiers, i.e., femtocell-to-macrocell, macrocell-to-femtocell [2]. Cross-tier interference is important, but not the only problem; co-tier interference between the cells within the same tier is also high likely to occur due to the facts such as plug and play feature of FAPs resulting in uncoordinated ad-hoc deployment, channel assignments, etc. Possible interference scenarios in a tiered network are illustrated in Figure 6.

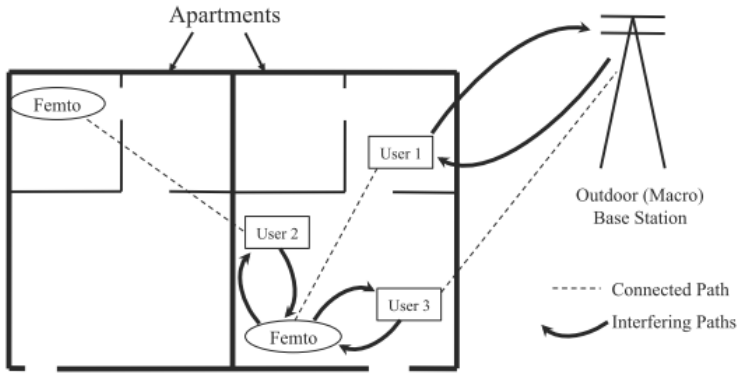

Figure 6: Interference scenarios in a tiered network

There are two important classifications for femtocells affecting the interference scenarios dramatically: Access control types and channel assignment schemes.

Access control There are three access control types for femtocells defined in the literature.

Closed access For a closed access femtocell, there is a certain number of pre-registered home/office users, also called Closed Subscriber Group (CSG), that the FAP is restricted to provide service only to them.

Open access Open access femtocells on the other hand, behave like macrocell base stations since they allow macrocell users to handover as well as the neighbouring femtocell users. This access method is the one mostly desired

by the service providers since it helps to reduce the macrocell traffic load and increase the coverage area.

Hybrid access There is also hybrid access method that is the combination of those two, based on the principle of allocating the femtocell capacity among the licensed (CSG) and the other users.

Channel assignment Two channel-based operating modes are listed here. A hybrid case can be also considered as a feasible operating mode.

Co-channel deployment In a shared spectrum network, femtocells labelled as co-channel use the same frequency bands with macrocell base stations. This scheme offers to use spectrum resources effectively, however it may cause a severe degradation in the system performance due to the interference to/from macrocell and neighbouring femtocells.

Dedicated channel deployment In a dedicated channel deployment, on the other hand, FAPs operate in the frequency bands allocated only for femtocells. This method can be also called spectrum partitioning between femtocell and macrocell tiers and even if avoids the cross-tier interference, it limits the amount of available spectrum for each tier and thus, is not efficient in terms of utilizing the spectrum.

In the following sections, first, different interference mitigation techniques, each designed as a solution to the aforementioned issues will be discussed. Thereafter related work as a result of a conducted literature survey is presented in order to give an idea of the solutions proposed previously.

2.5 Interference Mitigation Solutions

Femtocell is an innovative technology emerging in recent years, and accordingly novel interference management methods are required to be designed and used with this new

femtocell overlaid macrocell, i.e., tiered, networks. There are several facts about the nature of femtocells that are required to be considered while designing and proposing interference mitigation techniques.

First of all, femtocells resemble Wi-Fi technology in many ways, however they operate in licensed spectrum in contrast to Wi-Fi. Second, femtocell networks are overlaid macrocell networks as already mentioned. These two facts indicate that in such a tiered network where each tier provides service to its users operating at the same licensed spectrum simultaneously, cross-tier interference is inevitable. Proposed solutions should consider this issue with the limited spectral resources.

Another fact to take into account is that femtocell access points are plug and play devices and thus, they are deployed by subscribers which result in unplanned and uncoordinated ad-hoc deployment. This fact ensures that adaptability is one of the significant parameters designing interference mitigation algorithms for femtocell-macrocell networks. Unlike the traditional cellular network, femtocell network topology is not certain and is constantly changing, since a new FAP can be installed by an end user anywhere at any time. The algorithms should be able to highly adapt to these changes in the topology.

Scalability is also an important parameter in addition to adaptability. Number of deployed femtocells is expected to reach almost 50 million by 2014 [1]. This projected dense deployment of femtocells requires highly scalable interference mitigation solutions.

Last but not least, FAPs are small devices with limited computation and transmit power unlike the traditional mBSs. Therefore, complex interference management algorithms must be avoided.

Besides all these facts, it should be noted that femtocell networks are self-organized networks [20]. Because of the zero-touch feature of FAPs which is mentioned earlier, self-organization is essential for a FAP unit to make sure that it can function on

its own. Self-organization consists of self-configuration, self-optimization, and self-healing[2]. To explain briefly, self-configuration feature authorize a device to be able to start collecting its configuration parameters and do the auto-configuration work as the device is powered up. Self-optimization however, provides the device with continuous state of optimizing parameters such as transmit power, signalling, and frequency allocation in order to ensure active and adequate communication. There is also self-healing which is put into use when a failure or degradation in communication occurs. Self-healing ensures that the device finds corrective actions and continues operation applying them. In the light of this information, it can be seen that signalling, transmit power level and computations such as frequency allocation are the parameters which can be optimized during the operation. Hence, these are the parameters most widely used and tried to optimize for interference management solutions in the literature.

2.6 Related Work

There are many studies in recent literature which have been proposing interference management techniques for tiered networks concerning different scenarios. When the resulting solutions were examined, used techniques for proposed solutions can be categorized by two main and common approaches: spectrum management (spectrum splitting, frequency allocation schemes) and power control and summarized as follows.

Spectrum partitioning In multi-tier networks, spectrum partitioning is a technique used to divide the spectrum and dedicate the portions to different tiers. Since the technique provides dedicated channels to operate on to the tiers of the network, it is mainly used to fight cross-tier interference. How to split the spectrum in an optimum way has been an important research topic recently. There is a trade-off between higher capacity and interference. The solutions allowing higher sharing between tiers result in systems with higher capacity but more interference vulnerable. On the other hand, the solutions that provide fully

separated spectrum i.e., fully dedicated frequency bands to the tiers introduce more interference resistant systems but decreasing the system capacity. Hybrid solutions are also feasible as proposed in [21].

Power control This solution technique is used to calibrate the transmission power of base stations in order to mitigate the interference which might result from unnecessary high power. Power control can be used to manage both co-tier and cross-tier interferences.

Frequency allocation Due to the limited spectral resources, base stations must completely reuse the frequency resources. Accordingly, appropriate allocation of frequency channels to users is another solution to mitigate interference. Some of the proposed algorithms in this matter are adaptive Fractional Frequency Reuse (FFR) [22] and Dynamic FFR [23] which are mainly designed to mitigate co-tier interference in multi-femtocell environments.

The rest of this section presents the current interference mitigation solutions in order to familiarize the reader with the related studies from the literature.

Concerning spectrum management, an optimum decentralized spectrum partitioning strategy for two tiered networks has been proposed in [24] that gives the ratios of the spectrum allocation to the femtocell and macrocell tiers. A stochastic geometry framework to model the random spatial distribution of femtocells is employed as a contribution. The proposed spectrum allocation aims at maximizing the spatial reuse based on a network wide Quality of Service (QoS) condition ensuring a minimum expected throughput per user.

The authors in [25] study an OFDMA two tiered network employing universal frequency reuse focusing on mitigating downlink femto-to-macro interference. A dynamic frequency partitioning scheme that does not allow the HeNBs to access to downlink resources assigned to nearby macro cellular users is proposed in the paper.

Hence, interference to the most vulnerable macro UEs is effectively controlled at the cost of a small degradation in femtocell capacity, as far as the authors claimed.

In [26], a hybrid frequency assignment scheme has been proposed in which a dedicated, femtocell-only, frequency band is allocated to femtocells depending on the geographic positions of femtocells and macro base station (mBS). The idea is to split the femtocell overlaid macrocell coverage area into inner and outer regions. If a FAP is in the inner region, then it does not operate in a co-channel mode, instead it operates on a frequency band other than the one used by mBS. The authors also provided the calculation for best threshold that determines the inner and outer regions.

Similar study is done in [27] again proposes a hybrid scheme of frequency resource allocation, nevertheless it also adds clustering and power control algorithms to this scheme. A cluster is defined as the unit for frequency reuse among femtocells. Frequency bandwidth partitioning between femtocell and macrocell tiers is done by a step-migration-algorithm-based power control.

Careful analysis of these works shows that cross-tier interference is eliminated at the cost of spectrum efficiency more or less.

The implementation of power control mechanisms in two-tier networks could be considered as the other important interference mitigation method used in the literature. Since two fundamental features of WCDMA, variable spreading factor (SF) and *fast power control*, are disabled and replaced by several techniques including adaptive modulation and coding (AMC) and a fast retransmission strategy (HARQ) introduced in HSDPA technology, different power control mechanisms have been designed and proposed to mitigate the cross-tier interference and/or increase the system capacity.

In [28], an open-loop and a closed loop power control schemes are proposed where femto mobile stations decrease their transmit power to mitigate uplink interference to mobile base station. With the open loop approach, a femtocell user calibrates the maximum transmit power in order to avoid the cross-tier interference originated from

the femtocell user and keep it below a fixed interference threshold. With the closed loop power control, the maximum transmit power of the femtocell user is adjusted to fulfil an adaptive interference threshold which is derived from uplink interference at the mBS and noise level.

Another power control scheme is proposed in [29] focusing on the uplink and ensuring adequate cellular performance with a SINR adaptation technique. Each femtocell maximizes an objective function that is composed of a reward which is SINR dependent and a penalty based on the interference at the macrocell. For the cases in which the cellular user does not achieve its SINR target, a distributed algorithm is proposed in order to decrease SINR target of the strongest femtocell interferers in a progressive manner until the cellular SINR target is satisfied.

Other than the works on uplink power control, studies [30, 31, 32] present downlink power control mechanisms where basically femtocells calibrate their downlink transmit powers based on different approaches.

Different auto-configuration and self-optimization strategies in femtocell networks are discussed in [30], all based on altering pilot power of the femtocells. In this study, power control decisions are made depending on mobility events from surrounding users. Auto-configuration is defined as it is responsible for the initial configuration of the FAP whereas the presented self-optimization techniques provide continuous optimization of the configuration. Proposed auto power configuration methods are fixed power, distance based, and measurement based auto-configuration. After this initial stage, self-optimization is put into use. The proposed self-optimization approaches aim at minimizing the number of mobility events balancing the power level of the FAP. More detailed information on this study is presented in results section.

In [31] two power control schemes namely geo-static power control and adaptive power control where the latter aims at balancing the degradation in macrocell performance and the throughput of femto users are studied. In geo-static power control,

femtocell transmit power is based on the distance between FAP and mBS. On the other hand, the femtocell transmit power is adapted depending on the network target rates in adaptive power control scheme.

Another adaptive downlink power control for femtocells proposed in [32] is based on the channel quality indicator (CQI) reports which is the feedback procedure in FDD HSDPA network. In other words, the dynamic power control algorithm adjusts the downlink transmit power according to a pre-defined QoS target.

Furthermore, the comparison of open and closed access methods is also considered as an important topic in cross-tier interference mitigation for two-tier networks [33, 34]. Open access is proposed as a key requirement for co-channel deployment of femtocells in [33]. Another work [34] considers femtocell open access in a stochastic geometric setting. However, interference from other macro base stations and inter-femtocell interference are ignored. In contrast, this paper addresses closed access femtocells and takes into account both cross-tier and inter-femtocell interferences since the closed access is more likely to be implemented in reality.

In the next chapter, we are proposing a novel approach that combines a power control scheme based on overall interference from all channels with spectrum sensing procedure. The solution depends on spectrum sensing period, interference threshold, and power drop rate, all defined as a parameter of the proposed algorithm. The optimal combination of these parameters is found by multiple objective optimization and presents our solution to the interference problem. The proposed solution runs in decentralized manner, hence it is assumed that there is no need for a central entity to gather information from the FAPs and mBSs. On the contrary, the algorithm can be run by each FAP itself.

CHAPTER III

JOINT SPECTRUM SENSING AND POWER CONTROL ALGORITHM

This chapter first describes the problem context and then the proposed interference management algorithm in detail. In the first section we present system description and problem definition and then in the following sections we present the proposed solution and necessary definitions and formulations for comprehension. The proposed solution provides an increase in total system performance by an considerable increase in macrocell tier performance.

3.1 Introduction

3.1.1 System Description

This thesis is concerned with downlink interference mitigation in two-tier HSDPA networks which are composed of femtocell tiers and underlaying macrocell tiers. These statements essentially describe the environment that the proposed algorithm is run upon. The characteristics of the system environment are then given in detail as:

HSDPA System HSDPA Release 10 as a 3G downlink air interface technology which is reviewed in Section 2.3 is considered in this work.

Tiered Network The proposed interference mitigation algorithm is designed to support femtocell tiered macrocell networks. Therefore, it might not give the optimal solution in case of non-tiered deployments.

Downlink Only downlink interference is considered to mitigate in this thesis work.

Closed Access All the femtocells are assumed closed access so that only the pre-registered home/office users are able to get service from each FAP. Macro-cellular users and other femtocell users are not allowed to handover.

Co-channel Operation Instead of dedicated spectrum, shared spectrum where the bandwidth is shared between two tiers (macrocells and femtocells) is used in the system model.

3.1.2 Problem Definition

In the tiered network described previously, the main tier is the macro-cellular tier that includes mBSs deployed by operator at specific locations. Femto-cellular tier on the other hand, is user-deployed in an ad-hoc manner. There are UEs served by FAPs, thereby being referred to as femtocell user equipments (FUEs). UEs connected to mBSs however, are named as MUEs. As stated in Chapter II, in HSDPA each UE sends a CQI message to the base station at each TTI, depending on the measured HS-DSCH SINR. In other words, CQI is a function of SINR and maximum transport block sizes are denoted by CQIs, hence SINR is significant for the HSDPA data rate performances of UEs.

Small distances between FAPs and their FUEs result in relatively higher SINR whereas the MUEs in FAP-installed or neighbouring apartments suffers from low SINR values due to the aforementioned co-channel deployment and closed access FAPs. In this work, the problem of appropriate spectrum sensing and power control is investigated. An optimal combination of pre-defined independent variables that aims at maximizing the overall system capacity, is proposed.

3.2 Proposed Solution

Consider the aforementioned two-tier HSDPA network and the problem definition. In such an environment, spectrum partitioning is the first to be eliminated due to the

limited spectral resources. Therefore, femtocells must completely reuse the frequency resources with an optimal sensing period. However, it is observed that an optimal sensing procedure is not sufficient alone to save indoor MUEs and maximize the overall capacity. As a result, a power control scheme for FAPs is also required to consider as a part of the solution. The proposed interference management algorithm is a combination of the optimized spectrum sensing and power control processes. Before explaining the main procedure of the algorithm, it is essential to give some definitions of the parameters which are the backbone of the algorithm.

3.2.1 Independent Variables

In our interference management model there are three independent variables defined at the beginning and remain same during one simulation time. They are dramatically important since optimum combination of those three gives the optimum solution of our algorithm.

Sensing Period (SP) Since the spectrum is shared, each FAP is required to sense the spectrum and choose the frequency channel with minimum interference level in order to operate on. Sensing period is the certain period of time between the two spectrum sensing processes of a FAP.

Threshold (Th) There is a certain level of received interference that we name *interference threshold* and power control scheme significantly depends on it, because Th determines whether the transmit power of a FAP is reduced or not.

Drop Percentage ($\mathbf{P}_{drop}$) Every time a FAP senses the spectrum and compare the Th with the received interference levels from all channels, accordingly it decides whether it reduces its transmit power by a certain percentage of its current Tx power. This certain percentage is defined as drop percentage, P_{drop}.

These three parameters are crucial to understand the following sections.

3.2.2 Main Procedure of the Algorithm

Proposed joint spectrum sensing and power control scheme contains two major steps as the name implies. Actually, spectrum sensing encompasses the power control step, i.e., sensing process runs definitely in each sensing period while the power control might run based on the "threshold" condition. With the help of these two steps, a FAP chooses the frequency channel with minimum interference to operate and also adjusts its current transmit power in order to mitigate both co-tier and cross-tier interferences.

In the following, let f_k to denote the frequency channels where $k \in 1, ..., 4$. We assume all M mBSs operate on f_1 whereas FAPs are allowed to use all spectrum including f_1, meaning it is not a dedicated channel case. A femtocell access point, FAP_j, estimates the received signal powers from M mBSs and all the other N-1 FAPs regardless of their operational frequency, as $\{R_m^i\}_{i=1,...,M}$ and $\{R_f^j\}_{j\neq j, j=1,...,N}$. All these received signal powers are undesired i.e., interference for FAP_j.

After obtaining R_m^i and R_f^j, the FAP filters these $M + N - 1$ values according to their carrier frequency, hence the overall interference for $\{f_k\}_{k=1,...,4}$ could be calculated. Let $\{I_k\}_{k=1,...,4}$ denote these overall interferences. Thereafter, two steps of the proposed scheme is carried out as follows:

Step 1 : In each sensing period, FAP senses the spectrum and computes the overall interferences for each channel as discussed above. Then, at TTI_t the FAP chooses f_t, min-interference-channel, to operate for the time period from TTI_t to $\text{TTI}_t + SP$ based on the I_k values of TTI_{t-1}.

Step 2 : After assigning its operational frequency f_t to the FAP for one SP, $\{I_k\}$ is compared with a pre-defined threshold Th. If $\{I_k\}$ for at least one k, is lower than Th, then the FAP does not do power control. However, when all I values exceed the Th, power control is run for the FAP resulting in drop of the current

Algorithm 1 Joint Spectrum Sensing and Power Control

Require: R_m^i, R_f^j, f_{t-1}^j

procedure PC INCLUDED SS FOR FAP_j($R_m^i, R_f^j, f_{t-1}^j, Th, P_{drop}, SP$)
  $inc \leftarrow 0$
  for $t \leftarrow 0 : SP : t_{end} - SP$ **do** ▷ Use of sensing period (SP)
    for all j except the FAP itself **do**
      if $f_{t-1}^j = ch_1$ **then**
        $I_1 \leftarrow I_1 + R_f^j(t)$
      else if $f_{t-1}^j = ch_2$ **then**
        $I_2 \leftarrow I_2 + R_f^j(t)$
      else if $f_{t-1}^j = ch_3$ **then**
        $I_3 \leftarrow I_3 + R_f^j(t)$
      else
        $I_4 \leftarrow I_4 + R_f^j(t)$
      end if
    end for
    for all i **do**
      $I_1 \leftarrow I_1 + R_m^i(t)$
    end for
    $I_m =$min(I_1, I_2, I_3, I_4)
    $f_t^j = ch_m$
    if $I_k > Th$ for all k **then** ▷ Use of interference threshold (Th)
      if $P_f^j > P_{f_{min}}$ **then**
        $P_f^j \leftarrow P_f^j - P_f^j \times P_{drop}$ ▷ Use of drop percentage (P_{drop})
        if $P_f^j \leq P_{f_{min}}$ **then**
          $P_f^j \leftarrow P_{f_{min}}$
        end if
      end if
    end if
    for all timeslots from t to $inc \times SP$ **do**
      $f_{timeslot}^j \leftarrow f_t^j$
    end for
    $inc \leftarrow inc + 1$
  end for
end procedure

Tx power of the FAP by a pre-defined percentage P_{drop} if and only the current Tx power is not lower than the pre-defined minimum power level $P_{f_{min}}$.

Algorithm 1 shows the procedure more detailed. SS and PC denote spectrum sensing and power control respectively. It is certain that the number of "for" loops is

not as large as it is showed here in algorithm 1. Instead, matrix operations provided by MATLAB are exploited.

In this process of joint spectrum sensing and power control mechanism, the very first basic parameters required to be computed are $\{R_m^i\}_{i=1,...,M}$ and $\{R_f^j\}_{j\neq j,j=1,...,N}$ as obvious. These received signal powers are computed using the impairments introduced in a wireless channel that are explained in Chapter IV. Outdoor-to-indoor link considered for $\{R_m^i\}$ whereas indoor-to-indoor link is used for $\{R_f^j\}$. General formula can be shown as

$$R_{m,f}^t = P_{m,f}^t PL_{\substack{out-to-in,\\ in-to-in}}^{-1} \gamma^t |\beta|^t \tag{2}$$

PL here, stands for path loss and it may include also wall penetration according to the link, outdoor-to-indoor or indoor-to-indoor. γ is log-normal shadowing and β is the component coming from the multipath fading (Rayleigh fading), briefly. More detailed information on this formulation is given in Chapter IV.

R_m^i and R_f^j are required to be updated every TTI obviously, because of the time-varying components. Besides, even if P_m remains constant, P_f may be altered due to the power control. Afterwards it is straightforward to derive I_k from R_m^i and R_f^j.

Critical question here is what should SP, Th, and P_{drop} be in order to achieve our goal of ensuring that indoor cellular users are provided with the best possible data rates in a co-channel femtocell overlaid network? This question leads us to multiple-objective optimization part of our work.

3.2.3 Multiple-Objective Optimization

Multiple-objective optimization, introduced by Pareto is concerned with finding solutions to optimization problems with multiple objectives $F_{obj} = \{f_{o_1}, f_{o_2}, ..., f_{o_L}\}$. A solution is called Pareto-optimal if any of the objectives cannot be improved without sacrificing the other objectives for this solution [35]. In this work, we aim to

find Pareto-optimal solution for the best operating point considering the joint system performance.

Let us assume that our joint system performance problem consists of L objective functions which are all required to be minimized. In that case, a Pareto-optimal solution, $\eta*$, is said to present if there is no other possible solution, η, that could perform

$$f_{o_l}(\eta) \leq f_{o_l}(\eta*) \quad \forall l \in \{1, 2, ..., L\} \tag{3}$$

meaning, $\eta*$ is the best solution in terms of the joint benefit of all objective functions. In multiple-objective optimization (MOO), there is also an infeasible solution called "utopia point" [36] that minimizes all the objective functions at the same time. Briefly, the Pareto-optimal solution must have the shortest distance to the utopia point. Hence, MOO scheme can be described with the following stages:

1. Defining the objective functions

2. Normalization of the objective function f_{o_k}, for all k

$$f_{o_{k,scaled}} = \frac{f_{o_k} - f_{o_{min}}}{f_{o_{max}} - f_{o_{min}}} \tag{4}$$

   If the units of all L objective functions are the same, then this stage is dispensable.

3. Calculation of L-dimensional euclidean distance to the utopia point.

In a femtocell overlaid macrocell network, cellular subscribers and closed subscriber group of femtocells have to exist and get service from their serving mBS or FAP simultaneously. Our investigations indicate that the outdoor cellular users are not highly interfered by the existence of indoor femtocells while the cellular users who are indoor, in the apartment units with a FAP installed or in the neighbouring

apartment units, are severely interfered, thereby even losing the network connection. Hence, we aim to save the victim neighbouring MUEs from the violation of aggressor FAPs with the minimum possible damage on FUE data rate performance.

In consequence, we take these two objectives of minimizing the difference between the maximum possible data rate that a UE could achieve and the average data rates that both indoor MUEs and FUEs actually achieve, into account for our MOO framework. Then, we say there are two contradictory objective functions ($L = 2$) formulated based on the joint system performance. The contradiction leads to Pareto-optimal solution that is found by Eq. 3 to be required for the problem.

The Pareto-optimal solution in our case implies the combination of optimized algorithm parameters, SP, Th, and P_{drop}. Here, we explain the MOO work done to find the optimum operating point among all the operating points. An operating point essentially stands for the joint system performance obtained by using a unique combination of the algorithm parameters. In other words, at least one of the variables SP, Th, P_{drop} differ from one operating point to another.

The objective functions to be minimized are defined as;

$$f_{o_1} = T_{max} - T_{avg}^{indoorMUE} \tag{5}$$

$$f_{o_2} = T_{max} - T_{avg}^{FUE} \tag{6}$$

where T_{max} is the maximum achievable data rate, $T_{avg}^{indoorMUE}$ is the average data rate of the indoor cellular users, and T_{avg}^{FUE} is the average data rate achieved by femtocell users. Since both units of the objective functions are the same (Mbps), the second stage of MOO framework, normalization, is not necessarily applied.

Utopia point in this system is the point of (0,0), i.e., $f_{o_1} = f_{o_2} = 0$ which is the infeasible solution. As the last stage of the MOO scheme, two-dimensional euclidean distances to the utopia point are calculated for all operating points. The operating

point with the minimum euclidean distance to the utopia point, i.e., where all the objective functions are jointly minimized is the *optimum operating point*. Optimized SP, Th, and P_{drop} values are presented in Table 8, within the section of performance evaluation.

CHAPTER IV

SIMULATION-LEVEL MODELING

In this chapter, system and simulation-level models and parameters used in the extensive simulations are presented. Every detail from urban environment with apartment blocks to the information access patterns of femtocell users is taken into consideration in order to create a realistic simulation environment.

4.1 Two-Tier Network Model

In this work, a macrocell network where the central serving macrocell is overlaid with femtocells is considered. The system consists of M ($M-1$ of them are neighbouring) hexagonal macrocells with all having a coverage radius of r_m and the apartment blocks placed in the central macrocell, as depicted in Fig 7. Each mBS operates at a fixed transmit power of P_m. Within the coverage of the central macrocell, an urban environment is created with the blocks of apartments placed in specific locations. Each block represents two stripes of apartments where each stripe has 2 by 5. Each apartment unit is of size $10m$x$10m$ as convenient for urban case. There is a street between the two stripes of apartments, with width of $10m$. Every block has K floors where for each, K is chosen randomly between K_{min} and K_{max}. Illustration of a block is given in Fig 8(a).

N co-channel femtocell access points are then randomly deployed on the apartment units. The maximum and the minimum transmit powers of FAPs with an omni-directional antenna are denoted as $P_{f_{max}}$, $P_{f_{min}}$ respectively. Every femtocell consists of the FAP and FUEs. It is assumed that the number of FUEs for each femtocell is randomly chosen between $n_{FUE_{min}}$ and $n_{FUE_{max}}$. There are also MUEs which are again randomly dropped in the entire central macrocell area with a given percentage is

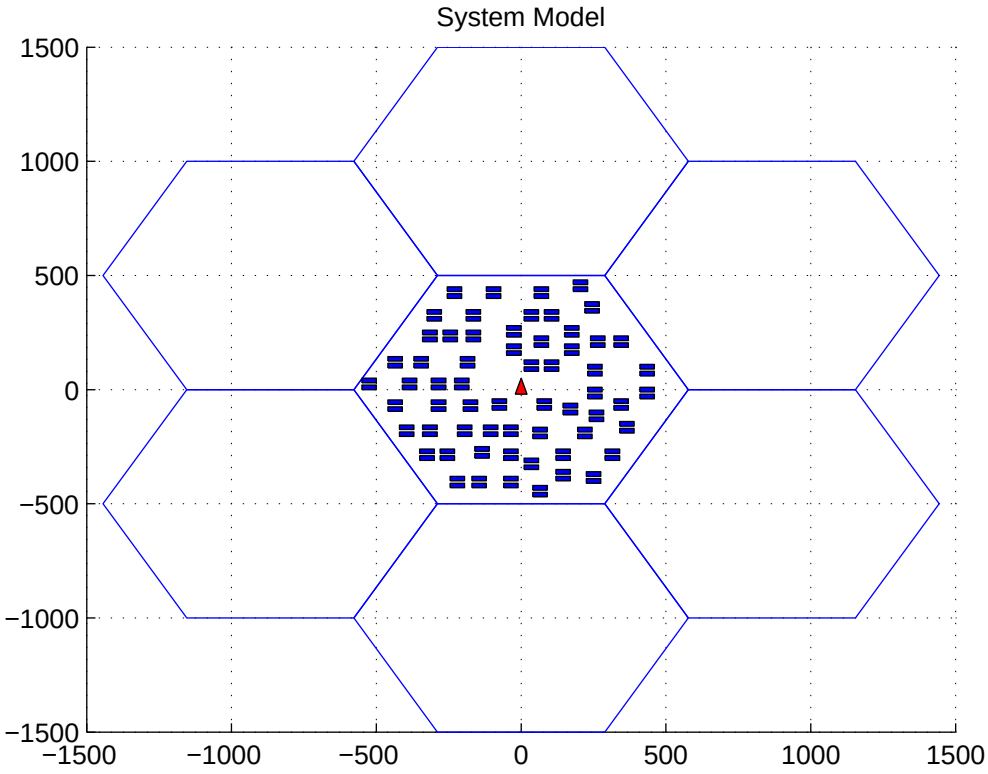

Figure 7: Network model

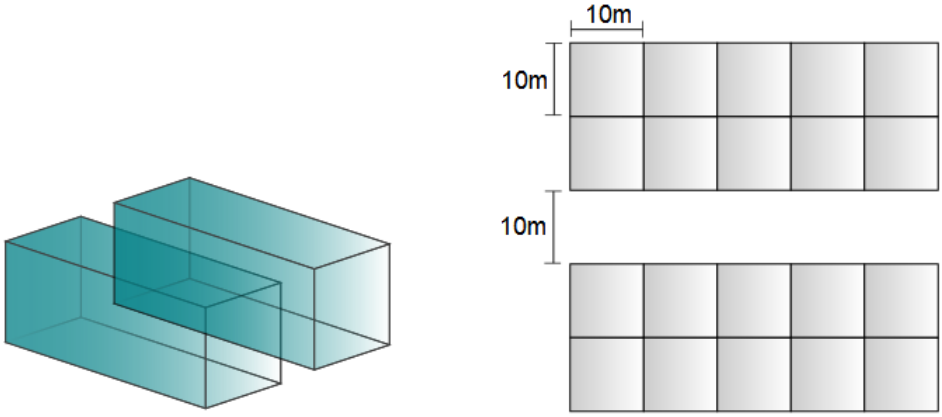

(a) 3-D view of one block in dense-urban model (b) Top view of one block in dense-urban model

Figure 8: One block of apartments in dense-urban model

indoor. We assume that the one-third of the indoor MUEs is in the apartment where a FAP is installed while the rest two-third of the indoor MUEs is in the apartments which have no FAP.

4.2 Information Access Patterns

As discussed, the majority of data services and even calls occurs indoors in cellular networks. Since we are interested in the Internet traffic rather than voice, we require to model indoor mobile information access patterns. According to the statistical study of Church et al. [37], information access modes could be categorized in terms of session types into two: browsing and search. To describe briefly, a mobile *browsing* session simply does not include a certain search action and the average number of this type of sessions is relatively high whereas an average *search* session time per user lasts longer and the average number of sessions is relatively low.

Accordingly, the femtocells deployed in our network model are divided into two in terms of session types as browsing FAP (we call it also "mobile usage FAP") and search FAP (also called "laptop usage FAP"). Hence, we assume that *all* the n_{FUE} users of a browsing femtocell are browsing on the Web and vice versa, since the distinction is made on the basis of femtocells. It is obvious that the average session times per user and the average number of sessions per day are different for these two kinds of femtocells. Table 4 shows these values obtained from the statistical work [37].

Table 4: Information Access Patterns for Different Type of Mobile Users

User type	Avg Number of Session per-day	Avg Session Duration (sec)
Browsing	1.8	278
Search	2.8	653

In the network model, we assume that 60% of the femtocells have browsing type FAPs while the rest 40% have search type FAPs. After assigning the session type

to a FAP, it is then known the corresponding $\lambda_{browsing}, \lambda_{search}$ and $\mu_{browsing}, \mu_{search}$, means of exponential random variables, that give the active and passive periods of the FAP in time. If a FAP is active, then it will transmit at full power. Otherwise, it will transmit only the pilot and overhead channels.

4.3 Wireless Channel

For a mobile radio channel, the dynamics of the environment are important as well as the structure of the receiver and transmitter. Moreover, thermal noise and interference make the condition and the parameters of the radio channel unpredictable. Typically, path loss, shadowing and multipath fading are the three main issues that cause some variations in the channel conditions. The radio propagation model we use for our simulations considers basically those three different parts.

In following sections, a summary on path-loss, shadowing and multipath fading models used in the thesis are presented.

4.3.1 Path Loss Models

The following five links are considered in path loss modelling.

Outdoor link , i.e., mBS to outdoor MUEs,

According to COST231 Walfisch-Ikegami non-line-of-sight model [38]:

$$PL = \begin{cases} L_{fs} + L_{rts} + L_{mds}, & L_{rts} + L_{mds} \geq 0 \\ L_{fs}, & L_{rts} + L_{mds} \leq 0 \end{cases} \tag{7}$$

where L_{fs} is the free space path-loss, L_{rts} is the roof-to-street diffraction and scatter loss, and L_{mds} is the multi-screen diffraction loss. Computations of these parameters are given as follows:

$$L_{fs} = 32.4 + 20\log(d) + 20\log(f) \tag{8}$$

$$L_{rts} = -16.9 - 10\log(w) + 10\log(f) + 20\log(\Delta h_m) + L_{ori} \tag{9}$$

where

$$L_{ori} = \begin{cases} -10 + 0.354(\phi), & 0 \leq \phi \leq 35^\circ \\ 2.5 + 0.075(\phi - 35^\circ), & 35^\circ \leq \phi \leq 55^\circ \\ 4.0 - 0.114 * (\phi - 55^\circ), & 55^\circ \leq \phi \leq 90^\circ \end{cases} \tag{10}$$

as an orientation loss, h_m is height of the mobile station, h_{roof} is the roof heights of buildings, $\Delta h_m = h_{roof} - h_m$, and w is the street width, all in meters.

$$L_{msd} = L_{bsh} + k_a + k_d\log(d) + k_f\log(f) - 9\log(b) \tag{11}$$

where

$$L_{bsh} = \begin{cases} -18\log(1 + \Delta h_b), & h_b > h_{roof} \\ 0, & h_b \leq h_{roof} \end{cases} \tag{12}$$

$$k_a = \begin{cases} 54, & h_b > h_{roof} \\ 54 - 0.8\Delta h_b, & d \geq 0.5kmandh_b \leq h_{roof} \\ 54 - 0.8\Delta h_b d/0.5, & d < 0.5kmandh_b \leq h_{roof} \end{cases} \tag{13}$$

$$k_d = \begin{cases} 18, & h_b > h_{roof} \\ 18 - 15\Delta h_b/h_{roof} \end{cases} \tag{14}$$

$$k_f = -4 + \begin{cases} 0.7(f_c/925 - 1), & \text{medium city and suburban} \\ 1.5(f_c/925 - 1), & \text{metropolitan area} \end{cases} \tag{15}$$

where h_b is mBS antenna height over street level and$\Delta h_b = h_b - h_{roof}$.

Throughout the thesis, we assume $h_b = 15$ m, $h_m = 2$ m, $h_{roof} = 12$ m, b = 20 m (building separation), w = b/2 , and $\phi = 90^\circ$ since we consider a metropolitan area.

Outdoor-to-indoor link , i.e., mBS to indoor FUEs and MUEs,

The mixed indoor outdoor environment model stated in [39] is used. According to this model, virtual positions of each users are to be calculated first. Each indoor receiver is projected to four virtual positions as illustrated in Figure 9. Attenuation is calculated using the outdoor link model between mBS and each virtual position, then the lowest path loss is selected for further calculations.

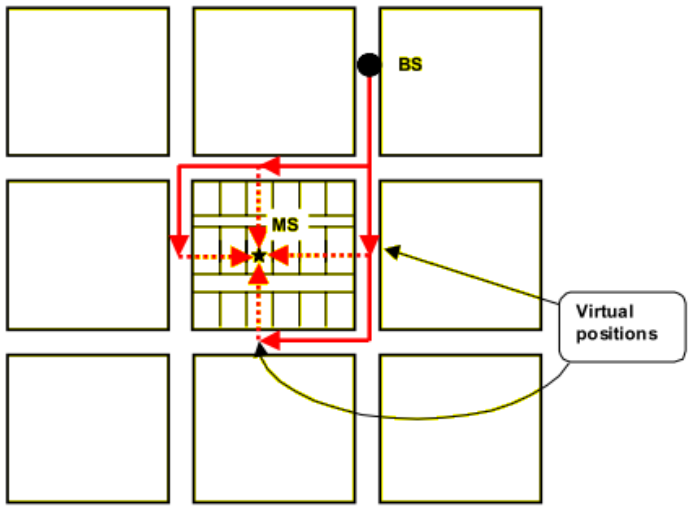

Figure 9: Virtual positions

Then, the path loss between outdoor transmitter and indoor receiver is calculated as

$$PL = PL^{v}_{macro} + aR + qW + L_{ow} \tag{16}$$

where PL^{v}_{macro} is the path loss from a mBS to the virtual UE, R is the distance between the actual UE and the virtual UE, q is the total number of walls between the actual UE and the virtual UE, W is the loss for internal walls, and L_{ow} is the loss for external wall. Here, a is the attenuation coefficient which is assumed 0.8 dB/m.

Indoor link , i.e., FAP to its serving FUEs and non-serving MUE/s in its femtocell,

Calculating the path loss for the indoor office environment we use COST231 Multi-wall Model assuming internal walls are not modelled individually. According to this model, path loss is stated in [39] as:

$$PL = 37 + 30 \log d + 18.3 n^{\frac{n+2}{n+1} - 0.46} \tag{17}$$

where d is the distance between transmitter and receiver, and n is the number of floors in the path.

Indoor-to-outdoor link , i.e., FAP to outdoor MUEs,

For this link we use the path loss model given in [40] as:

$$PL = PL_{fs} + qW + L_{ow} \tag{18a}$$

$$PL_{fs} = max(\text{Walfisch-Ikegami pathloss}, (37 + 20 \log d)) \tag{18b}$$

with d being the distance between the MUE and FAP in meters.

Indoor-to-indoor link , i.e., FAP to FUEs and MUEs in the different femtocells,

$$PL = max((15.3 + 37.6 \log d), (37 + 20 \log d)) + qW + 2L_{ow} \tag{19}$$

q in the equations denotes the total number of indoor walls between the transmitter and the receiver and since we assume that internal walls are not modelled individually, q is chosen randomly between 2 and 5.

4.3.2 Shadowing

By the nature of wireless channel, a transmitted signal might lose part of its power while propagating due to the obstruction by objects in the environment. This loss is a random process because of the dynamics of reflection, diffraction and scattering. Shadow fading, in particular, is large-scale fading which denotes the large-scale variations in the signal power resulting from the interaction with large objects.

In the literature, shadow fading is characterized by its one-dimensional distribution function that can be modelled as a log-normal distribution. We use a simple autocorrelation model for shadow fading proposed by Gudmundson [41] throughout this thesis, since this model is also taken into account in ITU-R Recommendation M.1225 [42]. Gudmundson's model is described in [38] as;

$$\Omega_{k+1(dBm)} = \zeta\Omega_{k(dBm)} + (1-\zeta)\nu_k \tag{20}$$

where $\Omega_{k(dBm)}$ is the mean envelope at location k, ζ is a parameter controlling the spatial correlation of shadow fading, and ν_k is a zero-mean Gaussian random variable with variance σ^2.

The spatial autocorrelation function of $\Omega_{k(dBm)}$ can be expressed as;

$$\Phi\Omega_{(dBm)}\Omega_{(dBm)}(n) = \frac{1-\zeta}{1+\zeta}\sigma^2\zeta^{|n|} \tag{21}$$

And the variance of the log-normal shadowing:

$$\sigma_\Omega^2 = \Phi\Omega_{(dBm)}\Omega_{(dBm)}(0) = \frac{1-\zeta}{1+\zeta}\sigma^2 \tag{22}$$

Therefore;

$$\Phi\Omega_{(dBm)}\Omega_{(dBm)}(n) = \sigma_\Omega^2\zeta^{|n|} \tag{23}$$

Considering these equations, shadow fading can be modelled using Gudmundson's model. In order to use the simulator in [41], it is required to relate the decorrelation parameter to the simulation index k. As stated in [38],[41] the envelope is sampled every T seconds, and in kT seconds, distance would be vkT where v denotes the velocity. Assuming ζ_D is the shadow correlation between two points separated by a distance D, autocorrelation function is given as;

$$\Phi\Omega_{(dBm)}\Omega_{(dBm)}(kT) = \sigma_\Omega^2\zeta_D^{(vT/D)|k|} \tag{24}$$

Shadow fading is simulated using this method of filtered Gaussian white noise according to parameters given in [41]. Furthermore, two different shadow standard

deviation; 8 dB (for outdoor) as a typical value for macro-cellular applications and 4 dB for indoors [33] are used in the simulations.

4.3.3 Multipath Fading

In mobile transmissions, the transmitted signal typically arrive at the receiver from many different directions and with different delays by being reflected at or scattered from different objects in the environment. Multiple reflected copies of the signal are combined at the receiver side and constructive - destructive manner of the combination results in multipath fading [38].

Multipath fading, unlike shadowing, takes into account the small-scale variations in the signal power which occur due to the movement of the transmitter and/or receiver. Furthermore, the movement of the mobile station introduces Doppler effect which is a shift in frequency, depending on the velocity of the mobile station v and the angle of incidence θ. The Doppler shift for n^{th} plane wave is given by

$$f_{D,n} = f_m cos\theta_n \quad \text{Hz} \tag{25}$$

where $f_m = v f_c/c$ and f_c is the carrier frequency (2000MHz), c is the speed of light, and f_m is the maximum Doppler frequency occurring when $\theta_n = 0$.

An urban environment is assumed for system simulations, therefore the envelope of the received signal can be modelled with a Rayleigh distribution considering that the possibility of existence of line-of-sight (LOS) component is so weak. Throughout the thesis, multipath fading is modelled using filtered Gaussian noise model and Clarke's scattering model both mentioned in [38]. In the model referred to as Clarke's 2-D isotropic scattering model, the Doppler power spectral density of the mobile channel is

$$S(f) = \frac{\Omega_p}{4\pi f_m} \frac{1}{\sqrt{1 - (\frac{f - f_c}{f_m})^2}}, \quad |f - f_c| \leq f_m \tag{26}$$

According to the filtered Gaussian noise model, the Rayleigh faded envelope is generated by filtering two independent white Gaussian noise sources with low-pass

filters. These filtered two noise sources are in-phase and quadrature parts of the Rayleigh faded envelope, namely r_I and r_Q. The two different noise sources r_I and r_Q must have the same power spectral density (psd) in order to produce a Rayleigh faded envelope. If they have the same psd of $\Omega_p/2$ Watts/Hz and the low pass filters have the same transfer function, H(f), then the auto and cross power spectral densities are given as:

$$S_{r_I r_I}(f) = S_{r_Q r_Q}(f) = \frac{\Omega_p}{2}|H(f)|^2 \tag{27a}$$

$$S_{r_I r_Q}(f) = 0 \tag{27b}$$

The low-pass filter $h(t)$ which is implemented as a first-order low-pass digital filter for discrete time simulations, models the fading process as a Markov process. When T is simulation step size, then at k^{th} simulation time $r_{I,k} = r_I(kT)$ and $r_{Q,k} = r_Q(kT)$. The state equation is then given as:

$$(r_{I,k+1}, r_{Q,k+1}) = \zeta(r_{I,k}, r_{Q,k}) + (1-\zeta)(\omega_{1,k}, \omega_{2,k}) \tag{28}$$

where $\omega_{1,k}$ and $\omega_{2,k}$ are two independent zero-mean Gaussian random variables with time autocorrelation $R_{\omega_{i,k},\omega_{i,l}} = \sigma^2\delta_{kl}, i$ =1,2. $r_k = r_{I,k} + jr_{Q,k}$ has zero-mean, the envelope $|r_k|^2$ is Rayleigh distributed and the phase $\phi_k = tan^{-1}(r_{Q,k}/r_{I,k})$ is uniformly distributed on the interval $[-\pi, \pi]$.

To complete the model, σ^2 and ζ are required to be specified so that the filter is designed to reproduce Clarke's Doppler power spectrum with frequency response

$$H(f) = \sqrt{\frac{\Omega_p}{4\pi f_m}\frac{1}{\sqrt{1-(\frac{f-f_c}{f_m})^2}}}, \quad |f - f_c| \leq f_m \tag{29}$$

It is possible to set the 3 dB point of $S_{r_I}(r_I)$ to $f_m/4$, resulting in

$$\zeta = 2 - \cos(2\pi f_m T) - \sqrt{(2 - cos(2\pi f_m T)^2) - 1} \tag{30}$$

Then the variance of two zero-mean Gaussian random variables can be written as:

$$\sigma^2 = \frac{\Omega_p}{2}\frac{1+\zeta}{1-\zeta} \tag{31}$$

Improved results for faded envelope can be obtained by using higher order filter instead of first-order low-pass filter. However, it will bring complexity to the simulator. As long as uncorrelated noise sources with same psd are needed to be used, a first-order filter is sufficient to simulate the Rayleigh fading. Throughout the simulations, a first-order digital filter that has a pole at ζ coming from Eq. 30 is used.

4.3.3.1 Pedestrian A Multipath Model

The received signal is then expressed with the combination of the effects of path loss, shadowing and Rayleigh fading as:

$$P_{r(dB)} = P_{t(dB)} + L_{p(dB)} + L_{s(dB)} + L_{R(dB)} \tag{32}$$

where $P_{r(dB)}$ is the received signal power, $P_{t(dB)}$ is the transmit signal power, $L_{p(dB)}$ is the path loss, $L_{s(dB)}$ is the loss due to shadowing and $L_{R(dB)}$ is the loss due to Rayleigh fading.

To produce a composite received signal by combining discrete propagation paths as shown in [38], following equation and ITU multipath model are used in the simulations:

$$R(t) = \sum b_i R_{r,i} u(t-\tau) \tag{33}$$

where i is the path index, b_i is the gain of the path and τ is the path delay. Since all the users in the simulations are assumed pedestrian, the ITU Pedestrian A multipath model shown in Table 5 [42] with user velocity of 3km/h is used for macro cellular users.

Another assumption in the simulations is that each MUE has a RAKE receiver with four fingers locking on to the four strongest resolvable paths. The receiver is

Table 5: Pedestrian A Multipath Model

Tap	Relative Delay (ns)	Average Power (dB)
1	0	0
2	110	-9.7
3	190	-19.2
4	410	-22.8

assumed to be able to resolve between two paths that have a delay more than a chip time. The chip time for HSDPA system operating at 3.84Mcps is approximately 260ns. The paths that are not resolvable are assumed to contribute with signal ratio based on the delay difference. The remaining resolvable paths contribute to the interference at the receiver. In the simulations, MRC (Maximum Ratio Combining) is assumed so that the received SINR is the sum of the SINRs of the four fingers of the RAKE receiver.

4.4 HSDPA Performance Analysis

Throughout the thesis, we consider a 3G WCDMA system and the expansion HSDPA Release 10 is assumed to be operational for packet data communications [43]. Necessary information on HSDPA is given in Section II. To briefly remind, there are several key technical enhancements introduced in HSDPA to improve downlink packet data in terms of capacity and throughput. Concept of link adaptation is important to be able to track the changes in link quality and to neutralize the effect of the instant variations. In HSDPA, link adaptation is applied using rate control which implies the process of adjusting the downlink bit rate by changing the modulation scheme, coding rate, and number of channelization codes according to the varying radio channel conditions of users.

One of the basic principles of HSDPA is the use of fast scheduling at NodeB which enables the dynamic resource allocation between users with the help of short

transmission time interval (TTI), 2ms. The scheduling decision of a user is done by a packet scheduler considering different aspects such as CQI report received from the UE, available resources, UE capabilities, data buffer status, and quality of service (QoS).

Each UE sends a CQI message to the Node B at each TTI. The CQI denotes the maximum transport block that the UE could receive at the current channel conditions. CQI values are integers between 0 and 30 where each integer corresponds to measured SINR of high speed downlink shared channel. In other words, downlink SINR is a key point concerning the HSDPA performance analysis, since the CQIs and correspondingly the HSDPA maximum data rate are presented as a function of average HS-DSCH SINR.

SINR calculation for HS-DSCH is performed by the formula [44]:

$$SINR = SF_{16}\frac{P_{HS-DSCH}}{\alpha P_{own} + P_{other} + P_{noise}} \tag{34}$$

where SF_{16} is the spreading factor, $P_{HS-DSCH}$ is the received power of the HS-DSCH which is 75% of the total power, P_{own} is the received own-cell interference, P_{other} is the received other-cell interference, α is non-orthogonality factor (0 if fully orthogonal), and P_{noise} is the received noise power.

This calculation of SINR is specifically used for performance of the femto-cellular user equipment (FUE) in the simulations since it is assumed the received signal arrives at receiver as single path and thus, α is 0 because of the orthogonality. For MUE performance on the other hand, ITU Pedestrian A multipath model that includes four paths is used and the HS-DSCH SINR computation is modified accordingly.

The measured SINR value is then mapped to a 5-bit CQI message by the UE. Among the different SINR-to-CQI mapping models stated in [45], we use the following model:

$$CQI = \begin{cases} 0, & \text{SINR} \leq -3.96 \\ \lfloor \dfrac{\text{SINR}}{1.02} + 4.81 \rfloor, & -3.96 < \text{SINR} < 26.04 \\ 30, & 26.04 \leq \text{SINR} \end{cases} \tag{35}$$

The corresponding block error probability (BLER) at this channel quality can be approximated as in [46]:

$$BLER = \{10^{2(\frac{\text{SINR} - 1.03\text{CQI} + 5.26}{\sqrt{3} - \log(\text{CQI})})} + 1\}^{\frac{-1}{0.7}} \tag{36}$$

Transport block size (TBS) denotes the maximum amount of data that can be transmitted in one TTI (2 ms) without exceeding a BLER of 10% in average [46]. CQI-to-TBS mapping is user equipment specific since the selection of an effective modulation scheme and coding rate which is referred to as transport format and resource combination (TFRC) for each UE does not only depends on the radio channel conditions but also the UE capability to support different link adaptation techniques mentioned earlier. Table 3 in Section II lists some of the UE categories specified in 3GPP Release 10 [18].

In the system model, all users are assumed to have equipments that belong to Category 14. In other words, the UE is capable to encode and decode all modulation schemes described within the HSDPA standard, as it is showed in Table 3. The mapping table for Category 14 type devices is given in Table 6.

Finally, the HSDPA data rate is calculated as it is stated in [46];

$$R_u = TBS.\frac{1}{2(ms)}.(1 - BLER) \tag{37}$$

Table 6: CQI to TBS Mapping for Category 14

CQI	TBS	Number of HS-PDSCH	Modulation
0	N/A	Out of range	Out of range
1	136	1	QPSK
2	176	1	QPSK
3	232	1	QPSK
4	320	1	QPSK
5	376	1	QPSK
6	464	1	QPSK
7	648	2	QPSK
8	792	2	QPSK
9	928	2	QPSK
10	1264	3	QPSK
11	1488	3	QPSK
12	1744	3	QPSK
13	2288	4	QPSK
14	2592	4	QPSK
15	3328	5	QPSK
16	3576	5	16-QAM
17	4200	5	16-QAM
18	4672	5	16-QAM
19	5296	5	16-QAM
20	5896	5	16-QAM
21	6568	5	16-QAM
22	7184	5	16-QAM
23	9736	7	16-QAM
24	11432	8	16-QAM
25	14424	10	16-QAM
26	15776	10	64-QAM
27	21768	12	64-QAM
28	26504	13	64-QAM
29	32264	14	64-QAM
30	38576	15	64-QAM

CHAPTER V

PERFORMANCE EVALUATION

This chapter describes software simulations and experimental work that have been done to quantify the performance of the proposed algorithm. Since the simulation models are given in the previous chapter in detail, this chapter presents the simulation setup briefly. However, evaluation metrics and their respective simulation scenarios are presented in detail, with scenario specific parameters and results.

5.1 Simulation Setup

We built an MATLAB based framework to simulate the different scenarios. The system under simulation is a two tiered HSDPA network. This network model described in section 4.1 has been used for the first simulations showing that this kind of wide area full of apartment blocks comprises more than 4000 apartment units and serves neither the goal of examining the co-tier interference nor the cross-tier interference. To be able to observe a severe co-tier interference, at least 3000 FAPs are required to be deployed in an environment with more than 4000 apartments; likewise the number of indoor MUEs is needed to be increased to examine the cross-tier interference as well. However, even 60 is a large number of FAPs when it comes to limited computation time. Thus, the number of blocks has been reduced since it is not feasible to increase the number of FAPs.

Therefore, subsequent simulations has been performed based on the topology in Figure 10 using the system simulation parameters listed in Table 7. The new topology is same with the one illustrated in Figure 7 in terms of 1-tier macrocell network, it differs only in terms of the number of blocks. The number of apartment blocks is reduced to one for two reasons: In order to be able to investigate the inter-femtocell

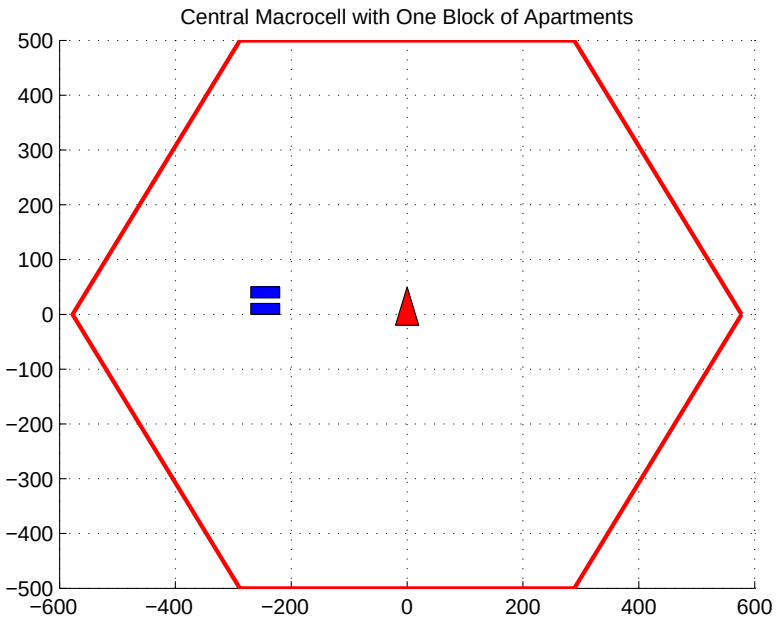

Figure 10: One block network topology

interference, we have seen that FAPs are required to be randomly deployed in the apartments that are *close* to each other. Furthermore, we have observed the most significant effect of co-channel deployment case is on the performance of indoor MUEs. It has been also stated in the previous chapters that we aim at saving the victim neighbouring/indoor MUEs from the violation of aggressor FAPs. Accordingly, we would rather indoor cellular users be in a block full of femtocells than be in neighbourhood of a few FAPs since the problem must exist before solving it. Then, that is the second reason we study on a case of one block of apartments in which N femtocells installed.

We have conducted extensive simulations to evaluate both the performance of the proposed joint spectrum sensing and power management algorithm and the optimization process.

In this chapter, we first give the Pareto-optimal solution of our interference management algorithm and evaluation of the system performance of the algorithm comparing its performance to two other schemes. Then, we present our study on the

Table 7: System Parameters

Symbol	Meaning	Value
M	Number of macrocells	7
N	Number of femtocells	25
P_m	Transmit power of mBS	43dBm
r_m	Radius of a hexagonal macrocell	577m
K_{min}, K_{max}	Number of floors for the block	2, 5
$P_{f_{max}}$	Max. transmit power of FAP	13dBm
$P_{f_{min}}$	Min. transmit power of FAP	-30dBm
$n_{FUE_{min}}$, $n_{FUE_{max}}$	Min. and max. number of subscribers of a FAP	1, 3
n_{MUE}	Total number of MUEs	30
-	Percentage of indoor MUEs	%30
NF	Noise figure at the UE and the FAP	7dB
f_c	Carrier frequency	2GHz
W	Channel bandwidth	5MHz
v	Velocity of pedestrian	3 kmph
SF	Spreading Factor	16
-	Number of rake fingers	4
R_c	HSDPA chip rate	3.84 Mcps
T_{max}	Max. achievable data rate for Category 14 device	19.288 Mbps

sensitivity analysis of the optimum operating point i.e., how sensitive it is to changes in the statistical λ and μ values.

5.2 Multi-Objective Optimization

As mentioned, we simulate a two-tier network using the parameter values given in Table 7. In a two-floor block (40 apartment units), 25 FAPs are deployed randomly with a uniform distribution. Each apartment with a FAP has also n_{FUE} chosen randomly between 1 and 3 and dropped in the area of $10m$x$10m$. The block is placed in the central macrocell, equidistant from the central mBS and the edge of the coverage area. %30 of the macrocell users are dropped indoors so that one-third of

these 9 indoor MUEs are in the FAP-installed apartments while the rest 6 MUEs are in FAP-free apartments.

Both the MUEs and FUEs are assumed pedestrian and dropped in their own areas (in the apartment units or outdoor) in every 2 minutes of the simulation time in order to obtain healthy results in the matter of geographical averaging. In this environment, the data rate performances of all users are computed as in Eq. 37 for each TTI according to the CQI_{TTI_t} which is a function of SINR_{TTI_t}. Then, the joint system performance is represented by the average data rates of the FUEs and indoor MUEs over time.

As all the FAPs are running the proposed algorithm explained in Section III with pre-defined SP, Th, P_{drop} values, average data rate performances of the FUEs and indoor MUEs, namely $T_{avg}^{indoorMUE}$ and $T_{avg}^{indoorMUE}$, are computed for each combination of SP, Th, P_{drop}. This is because our objective functions are based on the $T_{avg}^{indoorMUE}$ and $T_{avg}^{indoorMUE}$ values.

Totally, we have 567 combination where the independent variables SP, Th, P_{drop}, are swept in the intervals between 2min and 180min, 8×10^{-14}W and 1×10^{-12}W, and %10 and %90 respectively. Figure 11 depicts the optimum operating point that has the minimum euclidean distance to the utopia point (0, 0) among all 567 operating points.

The combination of the independent variables which is referred to as the optimum operating point or Pareto-optimal solution is represented in Table 8.

Table 8: Optimum Operating Point

Parameter	Optimum Value
SP	6 [min]
Th	1×10^{-13} Watt (-100dBm)
P_{drop}	%30

These values give the optimum solution considering both performances of cellular

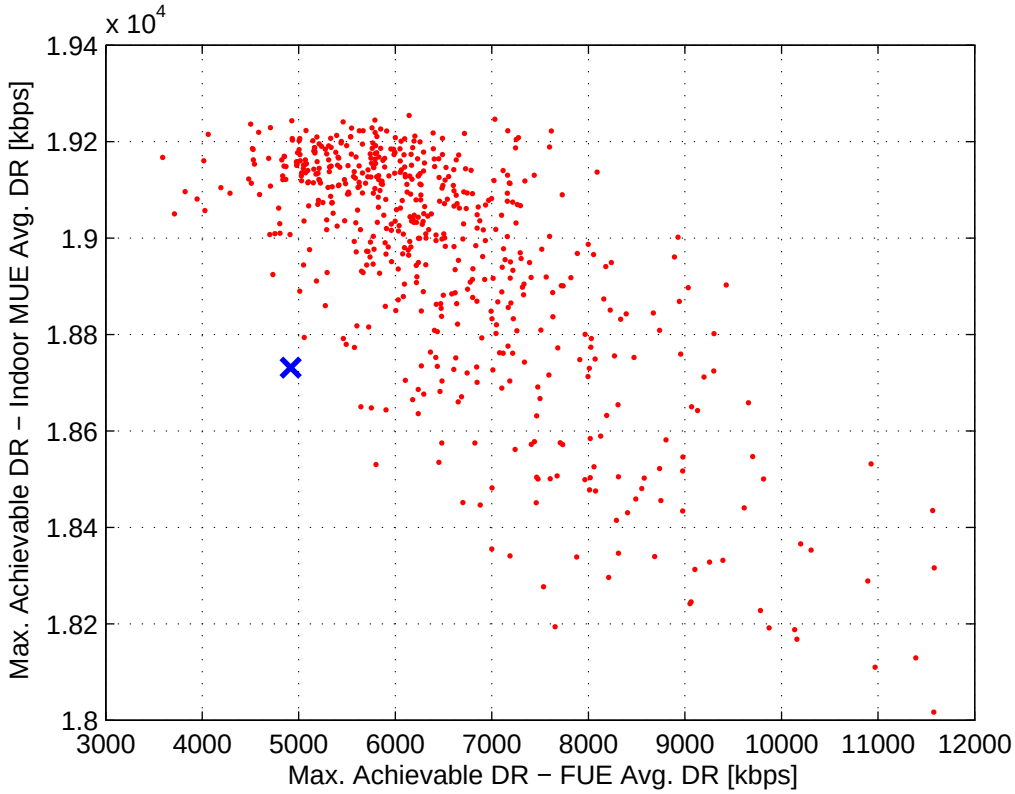

Figure 11: Optimum operating point

users and femtocell users. As it is depicted in Figure 11, Pareto-optimal solution minimizes the differences between maximum achievable data rate, T_{max}, and both the average data rate achieved by FUEs and the average data rate performance of indoor MUEs. Thus, the overall system performance is jointly maximized as intended.

Figures 12 and 13 depict the performances of femtocell and indoor cellular users when the optimum solution is used as an interference mitigation algorithm and when it is not in case of fully shared spectrum. SS and PC denote spectrum sensing and power control respectively. As shown in the figures, in a dense-femtocell environment such as more than 15 FAPs in a block of 40 apartment units, the proposed algorithm with optimized parameters provides a significant increase in overall system capacity by saving the indoor MUEs from the violation of FAPs. Furthermore, no degradation worth mentioning occurs in the data rate performance of FUEs while improving the

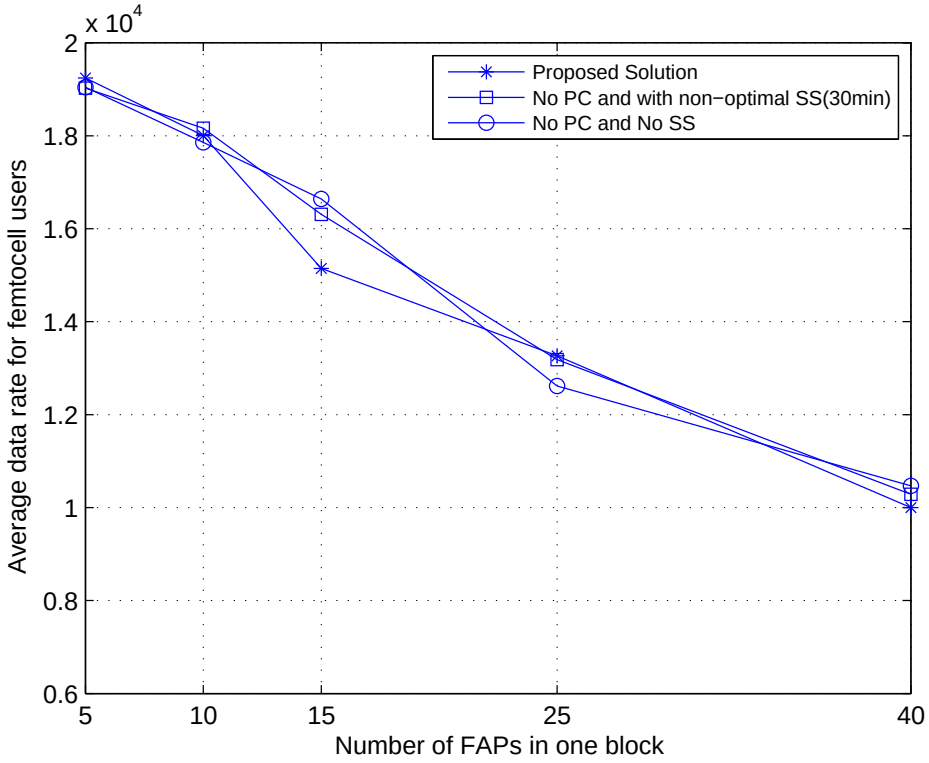

Figure 12: Performance of the femtocell users

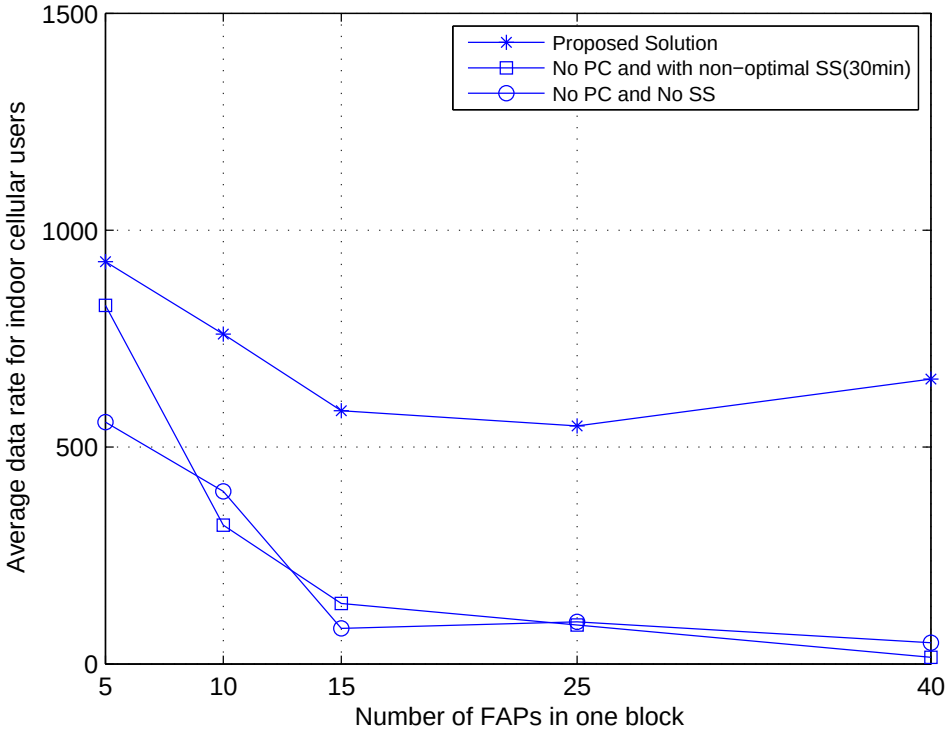

Figure 13: Performance of the indoor cellular users

performance of indoor cellular users.

5.3 Comparison with Candidate Algorithms

As discussed in the related work section in Chapter II, a comprehensive literature survey on interference management in two-tier networks has been conducted. Among these proposed solutions to the problem, the ones presented in [26, 30] have been chosen to be one reference example in each approach and contribute to evaluate the performance of the proposed algorithm. We carefully chose the techniques which fit best to our HSDPA network model as a solution to downlink interference scenarios and are also most cited. We run both schemes in our own environment with our own system-level parameters used.

5.3.1 Guvenc's Algorithm

To recall, Guvenc's algorithm proposed in [26] is a hybrid frequency assignment scheme that partitions the spectrum and performs the allocation depending on the geographic positions of FAPs and mBS. The procedure is implemented in our simulation environment as follows.

1. Determine if a FAP is in outer region or inner region. To do so, an ILCA (Interference Limited Coverage Area) for each femtocell which is defined as the area within a contour where the received powers from the FAP and mBS are the same is computed. If ILCA of a FAP is larger than a pre-defined threshold, then the FAP is assumed to be in outer region and vice versa.

2. Allow the femtocells which are determined in the outer region, for co-channel operation. On the other hand, femtocells in the inner region cannot use the frequency band that is used by the mBS.

Here, we assume that the threshold for comparison is 15 m since it was not specified in [26]. Moreover, Guvenc *et al.* assumed that the macrocell of interest use a different

frequency band from the neighbouring cells which in our case it does not. Spectrum sensing was also mentioned for minimizing the inter-femtocell interference, however neither the sensing period nor the sensing procedure was specified. Therefore, we use our optimum sensing period, 6 min, in the simulations.

Algorithm 2 Guvenc's algorithm

Require: $threshold, d$ ▷ $threshold(th) = 15m$

procedure DETERMINE WHETHER A FAP IS IN OUTER REGION(th, d)
  for all FAP **do**
    Find r where $P_{FAP} - PL_{indoor-to-outdoor}(r) = P_{mBS} - PL_{outdoor}(d - r)$
    $ILCA \leftarrow r$
    if $ILCA \geq th$ **then**
      $FAPregion \leftarrow outer$
    else
      $FAPregion \leftarrow inner$
    end if
  end for
end procedure

The algorithm for determining whether a FAP is outer region or not is also given in Algorithm 2 where d denotes the distance between the FAP and the mBS of interest. After the determination of the region of the FAP, it is straightforward: let co-channel operation if the FAP is in outer region, use a channel other than that used by mBS if the FAP is in inner region.

5.3.2 Claussen's Algorithm

Another approach is power control without any spectrum partitioning scheme. Claussen *et al.* [30] proposed different auto-configuration and self-optimization strategies in femtocell networks. Auto-configuration is defined as it is responsible for the initial configuration of the FAP whereas the presented self-optimization techniques provide continuous optimization of the configuration.

Three auto power configuration approaches are defined in [30] as follows.

Fixed power All FAPs start transmission with a fixed power. This is considered

the easiest approach of all, but obviously not the most efficient one.

Distance based A FAP starts transmission with a pilot power determined such that it is received as strong as the pilot power received from the strongest macrocell at a defined target cell radius. Received macrocell power is estimated using a path-loss model. If the maximum pilot power of the FAP is lower then the received mBs power then the initial pilot power of the FAP is the maximum pilot power.

Measurement based This method works as distance based one, but the difference is that the macrocell power is not estimated by a path loss model, rather is measured by the FAP.

After auto-configuration, self-optimization is put into use. The authors proposed a coverage adaptation technique for femtocell deployments which is called mobility event based self-optimization. Three different self-optimization methods were studied, however we, in this thesis, implement only one of them *"mobility event based-adapted to minimize mobility events of passing users"* as follows.

1. Initialize the pilot power of the FAPs using distance based auto-configuration scheme.

2. Count unwanted mobility events over time such as the hand-off attempts from the UEs who are not registered at the femtocell. If the number of unwanted mobility events exceeds a pre-defined value of n_1 events per time t_1, pilot power of the femtocell is reduced by Δ_1. On the other hand, pilot power of the femtocell is increased by Δ_2 if the number of unwanted events is smaller than or equal to a pre-defined n_2 events for a time period t_2.

All the values of the variables stated above are used as specified in [30]; $\Delta_1 = 3$dB, $\Delta_2 = 0.3$dB, $n_1 = n_2 = 0$ and $r_{femto} = 10$m. t_2 is set to a low value of 120s until a first

Algorithm 3 Claussen's Coverage Adaptation Algorithm

$P_{FAP_i,pilot} = min(R_{macro,pilot} + L_{femto}(r_{femto}), P_{pilot,max})$ ▷ Auto-configuration
$n_{unwanted} = 0$ ▷ Number of unwanted mobility events
for $t \leftarrow t_1 : t_1 : t_{end}$ **do**
    for all timeslot from $t - t_1$ to t **do**
        for all UE **do**
            if $Received_{FAP_i}$ at UE - $Received_{servingcell}$ at UE> 4dB **then**
                $n_{unwanted} \leftarrow n_{unwanted} + 1$
            end if
        end for
    end for
    if $t \leftarrow t_2$ **then**
        if $n_{unwanted} \leftarrow 0$ **then**
            $P_{FAP_i,pilot} \leftarrow P_{FAP_i,pilot} + \Delta_2$
        else
            $t_2 = 6(hour)$
        end if
    end if
    if $n_{unwanted} > 0$ **then**
        $P_{FAP_i,pilot} \leftarrow P_{FAP_i,pilot} - \Delta_1$
    end if
end for

unwanted mobility event occurs. Then t_2 is increased to 6h. t_1 on the other hand, is equal to the optimization iteration time and was not specified in [30]. Therefore, we specify several values for t_1 as 20s, 60s, 180s. The algorithm for the coverage adaptation method of Claussen *et al.* is given in Algorithm 3 where the distance based auto configuration scheme is used as initialization and $n_{unwanted}$ is the total number of hand-off attempts from MUEs and other FUEs in the time interval between $t - t_1$ and t .

Furthermore, we implement different cases where minimum power level for femtocells which was not specified in [30] is introduced and/or fixed power auto-configuration scheme is applied as an initialization method in the simulations.

Figures 14, 15 show the performance of the proposed algorithm compared with the aforementioned candidate algorithms of Guvenc and Claussen. Guvenc's algorithm provides spectrum partitioning without power control whereas the techniques

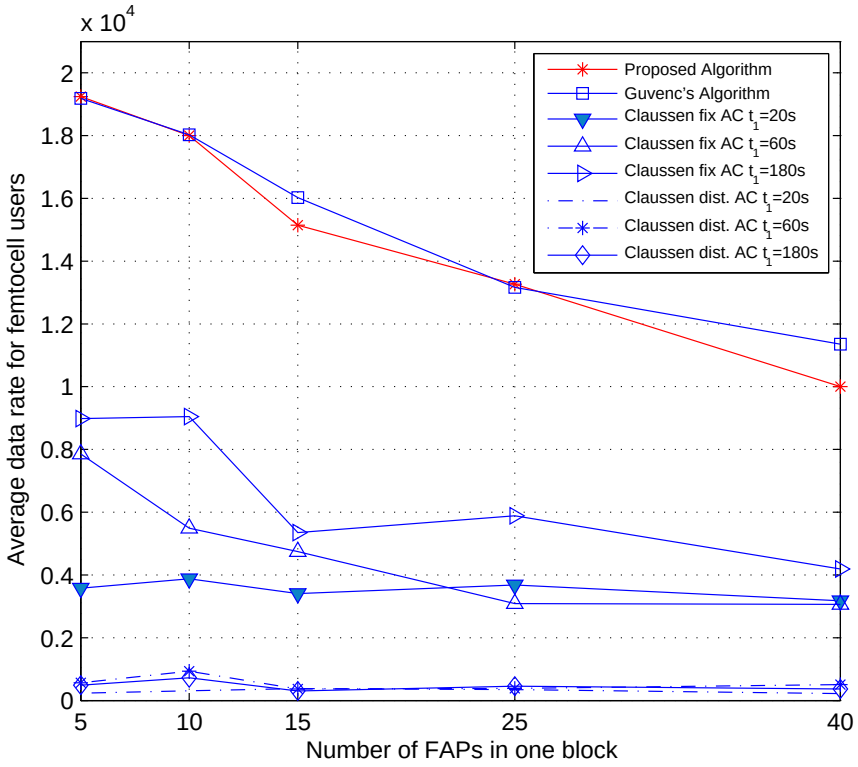

Figure 14: Performance of the femtocell users

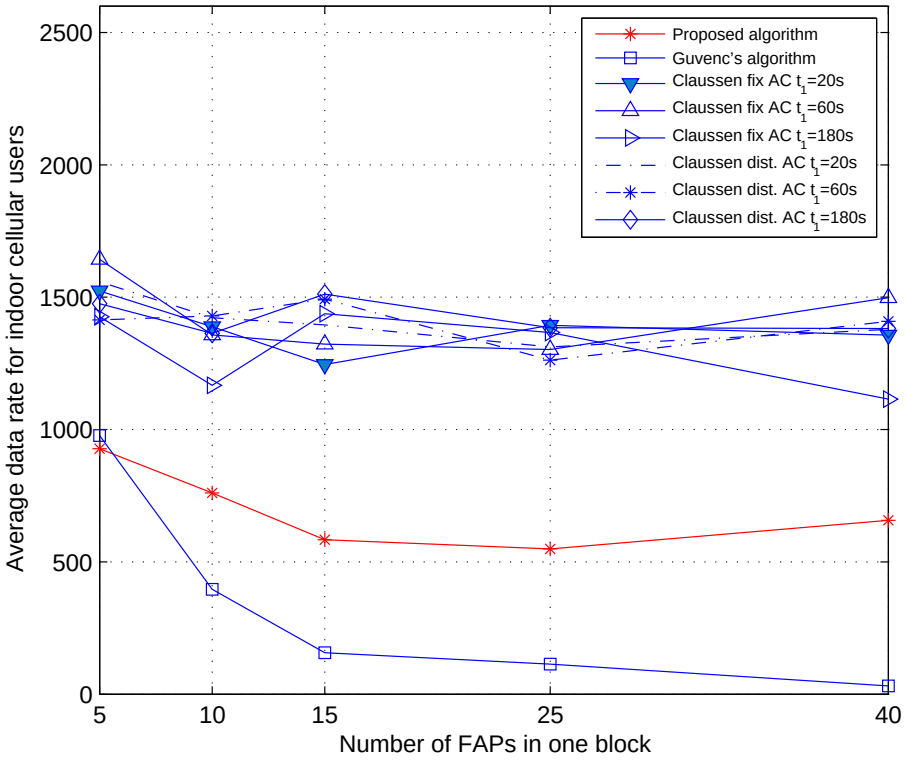

Figure 15: Performance of the indoor cellular users

proposed by Claussen introduce only power control without spectrum management. Our algorithm however, combines both.

Performances of the femtocell users and the macrocell users who are indoor for co-channel deployment are depicted in Figure 14 and 15 respectively. Two of the auto-configuration schemes, fixed power and distance based, proposed in [30] are implemented as initialization methods. In addition, the simulation is run for three different t_1 which was not specified by Claussen *et al.*. Therefore, there are 6 different cases implemented for Claussen's technique. Fix AC and Dist. AC denote fixed power auto-configuration and distance based auto-configuration respectively.

The self-optimization algorithm with fixed or distance based auto-configuration does not perform well in femtocell-tier even though it provides data rate to indoor cellular users as higher as dedicated case. Especially with distance based AC, FAPs reduce their transmit power even one unwanted mobility event occurs in t_1, hence they could not serve their subscribers as expected. This kind of solution might be useful in rural areas or at the edges of the macrocell coverage area.

Guvenc's algorithm on the other hand, performs well in femto-tier. It might even perform well in data rates of macro cellular users in some cases such as there is a few FAPs deployed in the block or the FAPs are distributed over the macrocell area so that there are long distances between them. However, in our case, urban environment with blocks of apartments, with lots of femtocell deployed, indoor MUEs still suffer from the violation of femtocells. Since the decision of co-channel operation for a FAP depends on the distance between the FAP and mBS, this algorithm might also work for the blocks closer to the mBS. However, this indicates that Guvenc's algorithm is not scalable or distributed and besides, it has many parameters to be specified and is open to improvements.

The proposed algorithm performs better in terms of overall system performance and scalability.

5.4 Sensitivity Analysis

An optimization process brings with it sensitivity issue of obtained optimum solution. In other words, it is required to study on how sensitive the optimum operating point is to the variances of the system parameters which are used to find it. In this section, we present the sensitivity analysis carried out for the optimum operating point given in section 5.2.

As mentioned earlier, we determined the values of $\lambda_{1,2}$ and $\mu_{1,2}$ based on a statistical study [37]. Small changes in these values are highly likely to occur in reality. Therefore, we have conducted series of simulations where $\lambda_{1,2}$ and $\mu_{1,2}$, mean values of the exponential random variables, were increased and reduced by a certain amount in order to study the sensitivity of the optimum operating point. Only one of the mean values were increased or reduced at a time while the others remained same. Accordingly, we had 15 different combination of $\lambda_{1,2}$, $\mu_{1,2}$ for one operating point, given in Table 9. Obviously, it is not sufficient to have the results for just the optimum operating point, however it is also time and resource consuming to re-simulate each one of 567 operating points for 15 different combinations. Therefore, we determined an area of interest as it can be seen in Figure 16.

It is not likely for the distant operating points to become optimum in case of small changes in $\lambda_{1,2}$ and $\mu_{1,2}$, hence to investigate the points in the area of interest i.e. that are closer to the current optimum point is more reasonable. The rectangular area depicted in the Figure 16 is the area of interest and there are 44 operating points including the current optimum. We rerun the simulations for these 44 operating points altering the $\lambda_{1,2}$, $\mu_{1,2}$ values.

It is seen that optimum operating point changes in most of the cases, however the performance achieved by the optimum points obtained is close to the one achieved by the original optimum. We have computed the deviations from the original optimum in the x-axis and y-axis, i.e. in the data rate performances of HUEs and indoor MUEs

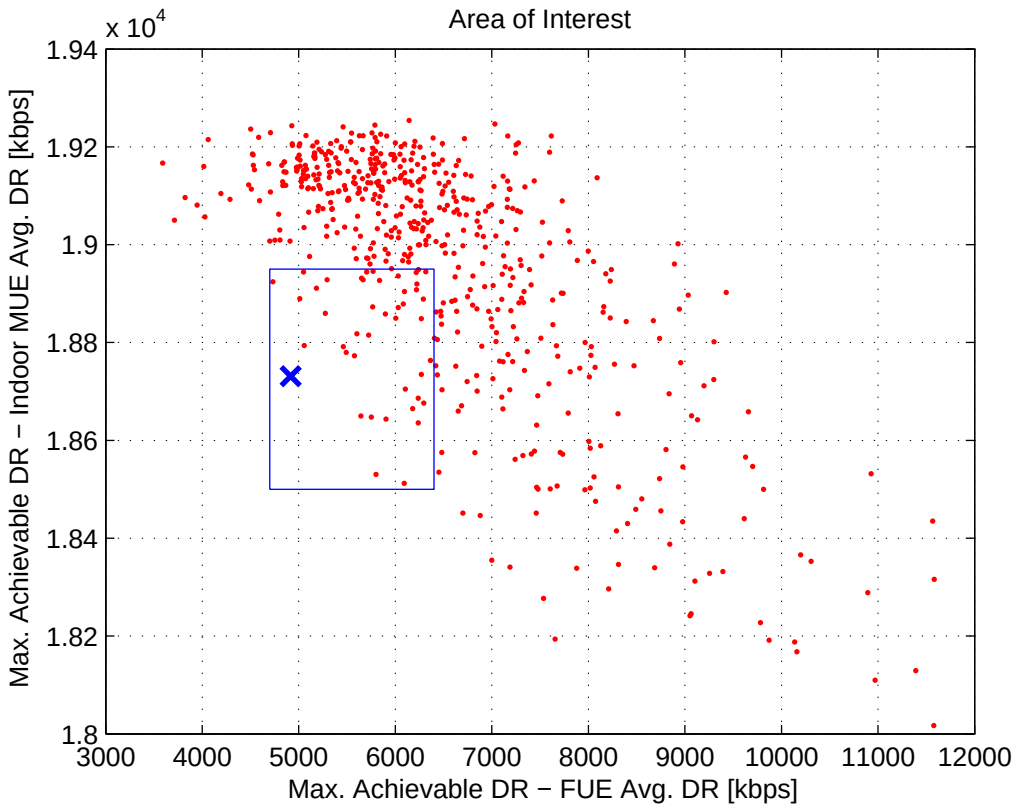

Figure 16: Area of interest

respectively. The results are tabulated in Table 9.

As can be seen, there is no improvement appeared on both sides in any case where negative number indicates the improvement and positive number indicates the decrement. This implies that non of the optimum points of these 15 cases performs better than the original optimum operating point concerning both FUE and MUE average data rate performances. Other than that, the deviations are really small (kbps) when they are compared with the actual data rate performances which are measured in Mbps.

In the light of the information on Table 9, the optimum operating point that gives the essential parameters of the proposed interference mitigation algorithm can not be said to be sensitive to the small changes in active-passive time periods.

Table 9: Sensitivity Analysis

Variations	Deviation in x (FUE performance) [kbps]	Deviation in y (MUE performance) [kbps]
$\lambda_1 - 150$	695.5547	-109.9473
$\lambda_1 + 150$	886.6877	-195.5237
$\lambda_1 + 300$	34.7966	34.0220
$\lambda_2 - 300$	414.7690	-117.3527
$\lambda_2 - 150$	846.5436	-133.8324
$\lambda_2 + 150$	646.0293	-89.0475
$\lambda_2 + 300$	-474.9633	272.5982
$\mu_1 - 400$	478.3739	-68.4034
$\mu_1 - 200$	419.6169	-18.4302
$\mu_1 + 200$	778.0092	-164.0246
$\mu_1 + 400$	274.2605	-77.9266
$\mu_2 - 400$	79.0907	6.9407
$\mu_2 - 200$	472.2227	52.0548
$\mu_2 + 200$	29.7468	114.4841
$\mu_2 + 400$	702.1942	-16.1878

CHAPTER VI

CONCLUSION

In this thesis, we proposed a joint spectrum sensing and power control algorithm to mitigate both cross-tier and co-tier interferences in a two-tier HSDPA network. On the contrary to the most of the studies of frequency partitioning spectrum allocation schemes, we considered an actual co-channel deployment where there is no spectrum splitting between tiers and thus provided high spectrum efficiency. Therefore, it is dramatically important that each FAP must sense the spectrum and employ the frequency band that has the lowest noise/interference floor in every certain period of time. Supported by extensive simulations, we observed that the cellular users who are in an apartment in a block where more than one FAP installed in different apartment units are highly interfered and even lose their network connection every so often. This shows us spectrum sensing is critical not only for the co-tier (inter-femtocell) interference, but also for cross-tier interference.

However, spectrum sensing alone is not sufficient to save the victim cellular users from the aggressor femtocells. Hence, we also proposed a power control algorithm for femtocells to adjust their transmit power depending on the received noise levels and operate jointly with spectrum sensing. Optimization of the algorithm parameters and sensitivity analysis of the optimum operating point are further works that are done throughout this thesis. Simulation results show that the proposed algorithm with optimized parameters provides a considerable increase in data rate performance of indoor cellular users even without causing a small performance degradation in femtocell-tier.

6.1 Future Work

Every detail to form a realistic environment has been considered in this thesis: Blocks of apartments, random deployment of FAPs, uniformly distributed subscribers and even mobile information access patterns meaning active and idle time periods of femtocells. The aforementioned promising results are obtained in such a detailed simulation environment for downlink interference scenarios. To investigate the uplink counterpart might be considered as a future work.

Bibliography

[1] J. Andrews, H. Claussen, M. Dohler, S. Rangan, and M. Reed, "Femtocells: Past, present, and future," *Selected Areas in Communications, IEEE Journal on*, vol. 30, pp. 497 –508, april 2012.

[2] J. Zhang and G. de la Roche, *Femtocells: Technologies and Deployment*. Wiley, 2011.

[3] S. Saunders, S. Carlaw, A. Giustina, R. Bhat, V. Rao, and R. Siegberg, *Femtocells: Opportunities and Challenges for Business and Technology*. Telecoms Explained, Wiley, 2009.

[4] A. Saleh, A. Rustako, and R. Roman, "Distributed antennas for indoor radio communications," *Communications, IEEE Transactions on*, vol. 35, pp. 1245 –1251, december 1987.

[5] J. Hoydis, M. Kobayashi, and M. Debbah, "Green small-cell networks," *Vehicular Technology Magazine, IEEE*, vol. 6, pp. 37 –43, march 2011.

[6] V. Chandrasekhar, J. Andrews, and A. Gatherer, "Femtocell networks: a survey," *Communications Magazine, IEEE*, vol. 46, pp. 59 –67, september 2008.

[7] J. Weitzen and T. Grosch, "Comparing coverage quality for femtocell and macrocell broadband data services," *Communications Magazine, IEEE*, vol. 48, pp. 40 –44, january 2010.

[8] J. Korhonen, *Introduction to 3G Mobile Communications*. Artech House Mobile Communications Series, Artech House, 2003.

[9] J. Bannister, P. Mather, and S. Coope, *Convergence Technologies for 3G Networks: IP, UMTS, EGPRS and ATM*. John Wiley & Sons, 2004.

[10] 3GPP Releases page. `http://www.3gpp.org/Releases`, 2012.

[11] J. Wannstrom, "Lte-advanced." `http://www.3gpp.org/lte-advanced`, May 2012.

[12] B. Walke, P. Seidenberg, and M. Althoff, *UMTS: the fundamentals*. Wiley, 2003.

[13] J. Gallego, A. Valdovinos, M. Canales, and J. de Mingo, "Analysis of closed loop power control modes in utra-fdd under time varying multipath channels," in *Personal, Indoor and Mobile Radio Communications, 2002. The 13th IEEE International Symposium on*, vol. 4, pp. 1616 – 1620 vol.4, sept. 2002.

[14] E. Dahlman, *3G Evolution: HSPA and LTE for Mobile Broadband*. Academic Press, Academic Press, 2008.

[15] H. Holma and A. Toskala, *HSDPA/HSUPA for UMTS: High Speed Radio Access for Mobile Communications*. Wiley, 2007.

[16] T. Nihtilä, *Performance of Advanced Transmission and Reception Algorithms for High Speed Downlink Packet Access*. PhD thesis, University of Jyväskylä, 2008.

[17] 3GPP Technical Specification Group Radio Access Network, "Physical layer - General description," TS 25.201 V7.2.0, 3rd Generation Partnership Project (3GPP), March 2007.

[18] 3GPP Technical Specification Group Radio Access Network, "UE radio access capabilities (release 10)," TS 25.306 V10.5.0, 3rd Generation Partnership Project (3GPP), December 2011.

[19] D. Chase, "Code combining–a maximum-likelihood decoding approach for combining an arbitrary number of noisy packets," *Communications, IEEE Transactions on*, vol. 33, pp. 385 – 393, may 1985.

[20] M. Bennis, L. Giupponi, E. Diaz, M. Lalam, M. Maqbool, E. Strinati, A. De Domenico, and M. Latva-aho, "Interference management in self-organized femtocell networks: The BeFEMTO approach," in *Wireless Communication, Vehicular Technology, Information Theory and Aerospace Electronic Systems Technology (Wireless VITAE), 2011 2nd International Conference on*, pp. 1 –6, 28 2011-march 3 2011.

[21] Y. Bai, J. Zhou, and L. Chen, "Hybrid spectrum sharing for coexistence of macrocell and femtocell," in *Communications Technology and Applications, 2009. ICCTA '09. IEEE International Conference on*, pp. 162 –166, oct. 2009.

[22] H.-C. Lee, D.-C. Oh, and Y.-H. Lee, "Mitigation of inter-femtocell interference with adaptive fractional frequency reuse," in *Communications (ICC), 2010 IEEE International Conference on*, pp. 1 –5, may 2010.

[23] M. Z. Chowdhury, Y. M. Jang, and Z. J. Haas, "Interference mitigation using dynamic frequency re-use for dense femtocell network architectures," in *Ubiquitous and Future Networks (ICUFN), 2010 Second International Conference on*, pp. 256 –261, june 2010.

[24] V. Chandrasekhar and J. Andrews, "Spectrum allocation in two-tier networks," in *Signals, Systems and Computers, 2008 42nd Asilomar Conference on*, pp. 1583 –1587, oct. 2008.

[25] Z. Bharucha, A. Saul, G. Auer, and H. Haas, "Dynamic resource partitioning for downlink femto-to-macro-cell interference avoidance," *EURASIP J. Wireless Comm. and Networking*, vol. 2010, 2010.

[26] I. Guvenc, M.-R. Jeong, F. Watanabe, and H. Inamura, "A hybrid frequency assignment for femtocells and coverage area analysis for co-channel operation," *Communications Letters, IEEE*, vol. 12, pp. 880 –882, december 2008.

[27] H. Li, X. Xu, D. Hu, X. Tao, P. Zhang, S. Ci, and H. Tang, "Clustering strategy based on graph method and power control for frequency resource management in femtocell and macrocell overlaid system," *Communications and Networks, Journal of*, vol. 13, pp. 664 –677, dec. 2011.

[28] H.-S. Jo, C. Mun, J. Moon, and J.-G. Yook, "Interference mitigation using uplink power control for two-tier femtocell networks," *Wireless Communications, IEEE Transactions on*, vol. 8, pp. 4906 –4910, october 2009.

[29] V. Chandrasekhar, J. Andrews, T. Muharemovic, Z. Shen, and A. Gatherer, "Power control in two-tier femtocell networks," *Wireless Communications, IEEE Transactions on*, vol. 8, pp. 4316 –4328, august 2009.

[30] H. Claussen, L. Ho, and L. Samuel, "Self-optimization of coverage for femtocell deployments," in *Wireless Telecommunications Symposium, 2008. WTS 2008*, pp. 278 –285, april 2008.

[31] N. Arulselvan, V. Ramachandran, S. Kalyanasundaram, and G. Han, "Distributed power control mechanisms for hsdpa femtocells," in *Vehicular Technology Conference, 2009. VTC Spring 2009. IEEE 69th*, pp. 1 –5, april 2009.

[32] M. Lalam, I. Papathanasiou, M. Maqbool, and T. Lestable, "Adaptive Downlink Power Control for HSDPA Femtocells," in *FUTURENET 2011, Future Network and Mobile Summit, 15-17 June 2011, Warsaw, Poland*, (Warsaw, POLAND), 06 2011.

[33] H. Claussen, "Performance of macro- and co-channel femtocells in a hierarchical cell structure," in *Personal, Indoor and Mobile Radio Communications, 2007. PIMRC 2007. IEEE 18th International Symposium on*, pp. 1 –5, sept. 2007.

[34] P. Xia, V. Chandrasekhar, and J. Andrews, "Open vs. closed access femtocells in the uplink," *Wireless Communications, IEEE Transactions on*, vol. 9, pp. 3798 –3809, december 2010.

[35] H. Ren, W. Zhou, N. Ken'ichi, W. Gao, and Q. Wu, "Multi-objective optimization for the operation of distributed energy systems considering economic and environmental aspects," *Applied Energy*, vol. 87, no. 12, pp. 3642–3651, 2010.

[36] T. Ozcelebi, M. Oguz Sunay, A. Murat Tekalp, and M. Reha Civanlar, "Cross-layer optimized rate adaptation and scheduling for multiple-user wireless video streaming," *Selected Areas in Communications, IEEE Journal on*, vol. 25, pp. 760 –769, may 2007.

[37] K. Church, B. Smyth, P. Cotter, and K. Bradley, "Mobile information access: A study of emerging search behavior on the mobile internet," *ACM Transactions on the Web (TWEB)*, vol. 1, no. 1, p. 4, 2007.

[38] G. Stüber, *Principles of Mobile Communication*. Springer New York, 2011.

[39] 3GPP Technical Specification Group Radio Access Network, "FDD Base Station (BS) classification," TR 25.951 V10.0.0, 3GPP, April 2011.

[40] 3GPP Technical Specification Group Radio Access Network WG4 44-bis, "HNB and HNB-Macro Propagation Models," R4 071617, 3GPP, October 2007.

[41] M. Gudmundson, "Correlation model for shadow fading in mobile radio systems," *Electronics Letters*, vol. 27, pp. 2145 –2146, nov. 1991.

[42] ITU-R , "Guidelines for Evaluation of Radio Transmission Technologies for IMT-2000," Recommendation M.1225, ITU-R.

[43] 3GPP Technical Specification Group Radio Access Network, "Physical Layer Procedure (FDD)," TS 25.214 V10.3.0, 3GPP, June 2011.

[44] "Interference Management in UMTS Femtocells," White paper 009, Small Cell Forum, February 2010.

[45] K. Freudenthaler, A. Springer, and J. Wehinger, "Novel sinr-to-cqi mapping maximizing the throughput in hsdpa," in *Wireless Communications and Networking Conference, 2007.WCNC 2007. IEEE*, pp. 2231 –2235, march 2007.

[46] M. Wrulich, W. Weiler, and M. Rupp, "Hsdpa performance in a mixed traffic network," in *Vehicular Technology Conference, 2008. VTC Spring 2008. IEEE*, pp. 2056 –2060, may 2008.

VITA

Gülden Ferazoğlu was born in Bursa, Turkey on October 3, 1988. She graduated from Bursa Karacabey Anadolu High School as valedictorian in 2006. She received her B.Sc. degree in Telecommunication Engineering with high honors from Istanbul Technical University in 2010. She joined Özyeğin University, Turkey in September 2010 where she worked as a teaching and research assistant until December 2012. She has been a recipient of the TÜBİTAK M.Sc. Fellowship during her M.Sc studies. She studied on *HSDPA, femtocells, tiered networks, interference management, multiple-objective optimization*. Her project was funded by Argela and her advisor is Assoc. Prof. Dr. M. Oğuz Sunay.